Available online at www.sciencedirect.com
SCIENCE DIRECT®
Icarus 166 (2003) 385–402
ICARUS
www.elsevier.com/locate/icarus

Blowing in the wind. II. Creation and redistribution of refractory inclusions in a turbulent protoplanetary nebula

Jeffrey N. Cuzzi,* Sanford S. Davis, and Anthony R. Dobrovolskis

Space Science Division, Mail Stop 245-3, Ames Research Center, Moffett Field, CA 94035, USA

Received 17 April 2003; revised 19 August 2003

Abstract

Ca–Al rich refractory mineral inclusions (CAIs) found at 1–6% mass fraction in primitive chondrites appear to be 1–3 million years older than the dominant (chondrule) components which were accreted into the same parent bodies. A prevalent concern is that it is difficult to retain CAIs for this long against gas-drag-induced radial drift into the Sun. We reassess the situation in terms of a hot inner (turbulent) nebula context for CAI formation, using analytical models of nebula evolution and particle diffusion. We show that outward radial diffusion in a weakly turbulent nebula can overcome inward drift, and prevent significant numbers of CAI-size particles from being lost into the Sun for times on the order of 10^6 years. CAIs can form early, when the inner nebula was hot, and persist in sufficient abundance to be incorporated into primitive planetesimals at a much later time. Small ($\lesssim 0.1$ mm diameter) CAIs persist for longer times than large ($\gtrsim 5$ mm diameter) ones. To obtain a quantitative match to the observed volume fractions of CAIs in chondrites, another process must be allowed for: a substantial enhancement of the inner hot nebula in silicate-forming material, which we suggest was caused by rapid inward drift of meter-sized objects. This early in nebula history, the drifting rubble would have a carbon content probably an order of magnitude larger than even the most primitive (CI) carbonaceous chondrites. Abundant carbon in the evaporating material would help keep the nebula oxygen fugacity low, plausibly solar, as inferred for the formation environment of CAIs. The associated production of a larger than canonical amount of CO_2 might also play a role in mass-independent fractionation of oxygen isotopes, leaving the gas rich in ^{16}O as inferred from CAIs and other high temperature condensates.
Published by Elsevier Inc.

Keywords: Origin, Solar System; Solar nebula; Meteorites; Mineralogy

1. Introduction

Chondrite parent bodies are dominated by particles with a surprisingly well-defined range of physical, chemical, and petrographic properties. Fe–Mg–Si–O mineral chondrules, many of which solidified from melted precursors stable at $T < 680$ K, constitute 30–80% of primitive meteorites. Most workers in the field believe that chondrules are formed by either localized or nebula scale energetic events operating on freely floating precursors of comparable mass, at some location or locations in the protoplanetary nebula (see, e.g., Grossman, 1989; Grossman et al., 1989; Boss, 1996; Connolly and Love, 1998; Jones et al., 2000; Desch and Connolly, 2002).

A different class of mineral objects called Ca–Al-rich inclusions (CAIs), whose constituent minerals condense out of nebula gas at a much higher temperature ($T > 1500$ K), make up 1–6% of primitive meteorites depending on CAI and chondrite type. Many, but not all, have apparently been subsequently melted (Grossman et al., 2002). The formation locale of CAIs is also unknown; some place it in the hot inner part of the terrestrial planet zone where the meteorites themselves subsequently evolve (e.g., Cassen, 2001), and others within a few stellar radii of the forming star (e.g., Shu et al., 1996). There is increasingly strong radioisotope evidence that most CAIs are several 10^6 years older than most chondrules (Mostefaoui et al., 2001; Huss et al., 2001; Amelin et al., 2002). How these high-temperature mineral fragments find themselves intimately mixed with lower-temperature minerals, especially after such a long time, has been regarded as a serious outstanding problem (e.g., recently, Alexander et al., 2001; Shukolyukov and Lugmair, 2002). In fact, some have even questioned the apparent age

* Corresponding author.
E-mail address: cuzzi@cosmic.arc.nasa.gov (J.N. Cuzzi).

0019-1035/$ – see front matter Published by Elsevier Inc.
doi:10.1016/j.icarus.2003.08.016

differences merely on the belief that CAIs would be lost by gas drag into the Sun in a time much shorter than the apparent age difference.

In this paper we address the survival of CAIs for times $> 10^6$ years. We show that radial diffusion counteracts the expected inward drift, given a certain amount of (weak) nebula turbulence. CAIs might form in the terrestrial planet zone—but early, at a high temperature—and resist inward drift processes for more than 10^6 years. CAIs might even form much closer to the Sun and still diffuse "upstream," radially outwards into cooler chondrule formation and accumulation regions. A combination of the two different source regions is both possible and consistent with the properties of the two main types of CAIs.

As part of this work, we describe a new process by which the inner solar nebula might become significantly enhanced in rock-forming elements, CO, and CO_2 relative to nominal abundances. The process is that of inward drift of very primitive, carbon-rich meter-sized particles into regions which are hot enough to evaporate them. Halley dust and cometary IDPs, for instance, have C/O ratios close to solar—that is, enriched by an order of magnitude relative to CI chondrites (Jessberger et al., 1988; Jessberger and Kissel, 1991; Lawler and Brownlee, 1992). Evaporation of this material along with ferromagnesian silicates allows the silicate abundance to increase without elevating the oxygen fugacity, as would occur for a nominal CI mix. Furthermore, Thiemens (1996, 1999) has argued that isotope exchange reactions involving CO_2 fractionate heavy oxygen isotopes into the CO_2, leaving reactive oxygen enriched in ^{16}O. The CO_2 is non-reactive at these temperatures, and carries the heavy isotopes away, leaving high-temperature condensates to become enriched in ^{16}O as observed. Quantitative development of these chemical and isotopic roles of carbon is beyond our expertise, so these aspects are not developed in detail but merely mentioned as plausibility arguments for others to pursue. In the remainder of this section we mention some basic aspects of turbulence, and of the influence of gas drag on particles. In Section 2 we describe our model which includes a globally evolving nebula, an inner nebula "CAI factory," and subsequent radial diffusion. In Section 3 we present our model results. In Section 4 we summarize and discuss the implications.

1.1. Turbulence

Weak global turbulence is an essential aspect of this scenario. It remains a subject of debate whether the nebula gas was turbulent or laminar during the CAI-chondrule era (Stone et al., 2000; Richard and Zahn, 1999; Klahr and Bodenheimer, 2002; Fleming and Stone, 2003; Richard, 2003). We have suggested that the typical chondrule size and size distribution themselves may be indicators of weak nebula turbulence (Cuzzi et al., 2001). In that paper, we also pointed out that adequate turbulence for interesting effects on particle evolution might be a *byproduct* of nebula evolution even if it is not a driver, and that only about 10^{-5} of the gravitational energy which is continually released as the nebula evolves needs to be tapped to generate this amount of turbulence. Turbulence can be described by its kinetic energy per unit mass $V_g^2/2$, and the sizes of its largest, or integral scale eddy L and its smallest, or Kolmogorov scale eddy η. The turbulent Reynolds number $Re = (L/\eta)^{3/4}$, is also written as $Re = \nu_T/\nu = V_g L/\nu = \alpha c H/\nu$, where ν_T and ν are the turbulent and molecular viscosities and H is the gas vertical scale height. V_g is the velocity of the large eddies, which contain most of the energy; the turnover time of these eddies, $t_L = 1/\Omega_L = L/V_g$, is generally assumed to be the orbit period. We will not distinguish here between the gas turbulent diffusivity $\mathcal{D}$ and turbulent viscosity ν_T (Prinn, 1990; Stevenson, 1990; cf. also Cuzzi et al., 2001, for more discussion). The smallest eddies have the smallest velocities and the shortest turnover times (Cuzzi et al., 2001; Cuzzi and Hogan, 2003). In reality, turbulence was probably radially, vertically, and temporally variable, but those specifics are beyond the scope of this paper, if not of current understanding; here we adopt two very simple, analytical models of turbulent intensity and viscosity which we expect will span a sufficiently wide range of behavior to provide insight into what may have happened in the actual nebula (discussed in Section 2). First, we sketch below the particle–gas dynamics involved.

1.2. Particle drift and diffusion

Particles such as CAIs and chondrules, which are smaller than the gas molecular mean free path, have a gas drag stopping time

$$t_s = r_p \rho_s / c \rho_g, \tag{1}$$

where r_p is particle radius, ρ_s is particle material density, c is the nebula sound speed, and ρ_g is the nebula gas density (Weidenschilling, 1977). Particles equilibrate with gas velocities on the timescale t_s. For CAIs and chondrules, and canonical nebula parameters, $t_s/t_L \equiv St \ll 1$. The value of St (the Stokes number) determines the interaction of the particles with a turbulent gas (Völk et al., 1980; Markiewicz et al., 1991; Cuzzi et al., 1993; Cuzzi and Hogan, 2003).

Weidenschilling (1977) presented radial drift velocities and lifetimes for various size particles in a number of *nonturbulent* nebula models, neglecting collective effects of adjacent particles (see however Nakagawa et al., 1986; Cuzzi et al., 1993). The angular velocities of small particles ($St \ll 1$) are forced to nearly match that of the gas, which orbits more slowly than Keplerian because it experiences a net outward pressure gradient acceleration $\Delta g = \frac{1}{\rho} dP/dR$. Thus, small particles experience an uncompensated inward acceleration Δg and acquire an inward drift velocity of

$$V_d = \Delta g t_s = -\frac{1}{\rho}\frac{dP}{dr} t_s \approx -2\gamma \frac{V_K^2}{r} t_s, \tag{2}$$

where γ is the ratio of the pressure gradient to the central force gravity and V_K is the Keplerian velocity. It turns out that $\gamma \approx 2 \times 10^{-3}$ is valid for a wide range of plausible nebula locations and conditions (Cuzzi et al., 1993). Then

$$V_d \approx -\frac{2\gamma V_K^2}{r} t_s \approx -\frac{2\gamma V_K^2 t_s \Omega}{r\Omega} \approx -2\gamma V_K t_s \Omega \approx -2\gamma V_K St \quad (3)$$

in the regime of interest where $\rho_d \ll \rho_g$ (cf. Nakagawa et al., 1986, Eq. 2.11). Thus, for small particles, V_d increases with St, until $St \sim 1$. The most rapidly drifting particles are those with $St = 1$; these drift at $V_d = -\gamma V_K$ (e.g., Weidenschilling, 1977). It happens that unit density, meter-radius particles satisfy $St \sim 1$ nearly throughout the entire nebula, because variations in Ω and drag coefficient offset variations in ρ_g. We refer to the drift velocity of "large" meter-sized particles as $V_L = -\gamma V_K$. For very large particles with $t_s \Omega = St > 1$, the drift velocity again decreases, as $V_d = -2\gamma V_K / St$.

The second effect of relevance is that the gas within which the particles are drifting is itself evolving radially due to angular momentum transfer. Lynden-Bell and Pringle (1974; henceforth LBP) showed that inner regions evolve inwards (into the Sun) and outer regions evolve outwards (conserving angular momentum), with the boundary between these regions itself evolving outwards with time. In our actual models (Section 2), we will use the analytical, radially dependent results of LBP, but for background purposes in this section the radial drift of the nebula gas V_n may be approximated by an inward velocity

$$V_n = -\frac{3}{2}\frac{\nu_T}{r} = -\frac{3}{2}\frac{\alpha c H}{r} = -\frac{3}{2}\alpha V_K \left(\frac{H}{r}\right)^2 \quad (4)$$

(Lin and Papaloizou, 1985; Cassen, 1996, 2001; Gail, 2001). For nebula parameters, both V_d and V_n are in the 10 cm/sec range (discussed in more detail below).

The third effect (if turbulence is present), is radial diffusion of the particles. The random inertial space velocity of the particles V_p determines the particle diffusion coefficient $\mathcal{D} = \nu_T V_p^2 / V_g^2$; Völk et al. (1980) and Cuzzi and Hogan (2003) show that $V_p^2 = V_g^2/(1+St) \approx V_g^2$ to a very good approximation for CAIs and chondrules, so $\mathcal{D} = \nu_T/(1+St) \approx \nu_T$ (see also Cuzzi et al., 1993, Appendix B). That is, because the stopping times of mm-sized particles are so much shorter than the turnover times of the most dispersive eddies, the velocity and mixing lengthscales of these particles are comparable to those of gas molecules.

A quick comparison of these three characteristic velocities reveals that V_p is much larger than either V_n or V_d for mm-to-cm-sized particles in the regime of interest. Specifically, for these particles $V_p \approx V_g = c\alpha^{1/2}$ (e.g., Cuzzi et al., 2001). For nebula α in the range of 10^{-4} to 10^{-2}, the random, turbulence-driven particle velocities V_p are much larger than drift velocities due to either gas drag or inward nebula evolution (V_p/V_d and V_p/V_n both $\sim 10^2$–10^4).

The main point is the radial *mass flux* of particles under either diffusion or advection. Suppose the vertically averaged CAI concentration C decreases outwards, with a radial lengthscale λ, as expected if CAIs form in some hot inner region. Then the ratio of (outward) diffusive flux to (inward) advective mass flux is

$$\frac{\mathcal{D}\sigma(\partial C/\partial r)}{(V_n + V_d)\sigma C} \sim \frac{\mathcal{D}\sigma(C/\lambda)}{V_n \sigma C} \sim \frac{r}{\lambda}, \quad (5)$$

where we have made use of the fact that $V_d \approx V_n$ for mm-sized particles, and have substituted $V_n \approx \mathcal{D}/r$ (Eq. (4)).

Equation (5) shows that diffusive (outward) mass flux dominates advective (inward) drift until the radial scale of variation of the concentration is larger than the radius itself—essentially, a nearly constant radial concentration profile. It is no more meaningful to discuss radial evolution of such particles without considering radial diffusion than it is to discuss "settling to the midplane" of such small particles without considering vertical diffusion (Dubrulle et al., 1995; Cuzzi et al., 1993, 1996). Indeed, Weidenschilling (1977) mentions some caveats on this subject, and it has also been discussed in detail by Morfill and Völk (1984), but with an approach that suppresses the radial transport aspects we wish to emphasize. In related research, Bockelèe-Moravan et al. (2002) used a full numerical diffusion-advection model to show that tiny grains from the inner Solar System, which do not incur appreciable gas-drag radial drift, diffuse throughout the Solar System on short timescales.

2. Method of solution

As a first step towards a solution of this complex problem, we frame a scenario for the "CAI factory" and adapt analytic solutions already in the literature to assess how the distribution of these particles evolves radially with time. We first describe our analytical nebula models (Section 2.1) and our scenario for the CAI factory, including the new aspect of drift enhancement of the inner regions in silicates (Section 2.2). We then describe how we treat simultaneous drift and diffusion (Section 2.3). We present typical results of the model in Section 3.

2.1. Nebula evolution

We must allow for the fact that, over the few $\times 10^6$ year duration of interesting evolution, the mass density and radial velocity of the nebula will evolve significantly by virtue of angular momentum and mass redistribution. We use the LBP analytic solutions for the radial profile of the local surface mass density $\sigma_g(r,t)$ and the nebula radial evolution velocity $V_n(r,t)$ in an evolving nebula. With the exception of the short-lived, hot inner region, we assume that silicates represent a constant fraction of the gas surface density.

The LBP formalism allows for a variety of powerlaw radial profiles of $\nu_T = \alpha c H = \alpha c^2/\Omega$ (see also Hartmann et

al., 1998). We choose two limiting cases; case 1 is a constant viscosity case $\nu_{T1} = \alpha c^2/\Omega_D$ and case 2 only has constant αc^2, which results in $\nu_{T2} = \alpha c^2/\Omega_D (r/r_D)^{3/2} \propto r^{3/2}$. Ω_D is the orbit frequency at a reference disk radius r_D defined below.[1] These two cases bracket a range of plausible r-dependencies of ν_T. R. Bell (personal communication, 2002) has found that, in her nebula energetics models (Bell et al., 1997), the radial dependence of visosity is actually not too far from one or the other of these dependencies (over different radial regions, the boundary between which changes with time). The LBP solutions may be exactly rewritten in simpler forms. For constant ν_T:

$$\sigma_1(r,t) = \left(\frac{M_D}{\pi r_D^2}\right)\left(1+\frac{t}{t_e}\right)^{-5/4} \exp\left[-\frac{(r/r_D)^2}{(1+t/t_e)}\right], \quad (6)$$

$$V_{n1}(r,t) = -\frac{3\nu_T}{2r}\left[1-\frac{(r/r_D)^2}{(1+t/t_e)}\right], \quad (7)$$

and for constant αc^2:

$$\sigma_2(r,t) = \left(\frac{M_D}{4\pi r_D^2}\right)\left(\frac{r}{r_D}\right)^{-3/2}\left(1+\frac{t}{t_e}\right)^{-2} \times \exp\left[-\frac{(r/r_D)^{1/2}}{(1+t/t_e)}\right], \quad (8)$$

$$V_{n2}(r,t) = -\frac{3\nu_T(r_D)}{2r}\left(\frac{r}{r_D}\right)^{3/2}\left[1-\frac{(r/r_D)^{1/2}}{(1+t/t_e)}\right]. \quad (9)$$

In the above equations, M_D is the initial disk mass, $M_\odot$ the solar mass, and G is the gravitational constant. The reference radius r_D is obtained using the angular momentum per unit mass scaling of Cassen (1996): $r_D = h_o^2/GM_\odot$, with h_o the specific angular momentum of the Solar System. The disk evolutionary timescale is $t_e = r_D^2\Omega_D/b\alpha c^2$, with $b = 12$ for the constant ν_T case and $b = 3/4$ for the constant αc^2 case. These equations may be of general use, since we have converted the arbitrary mathematical constants of LBP into three meaningful physical properties of the disk: M_D, r_D, and α. Specifically, we make the following substitutions for LBPs a and C: $a = (GM_\odot r_D)^{-2}$ (relating radii to the nebula's specific angular momentum); and $C/\nu_T = 3M_D/r_D^2$ (from integrating over the disk mass). A more complicated analytical model, although essentially based on the same three parameters, has been developed by Stepinski (1998). Davis (2002) also describes several different approaches to analytic modeling.

Typical results from such models are shown in Figs. 1–4, and model parameters are given in Table 1. In all figures, the constant viscosity models are shown in solid lines and the constant αc^2 models in dashed lines. In spite of the significant differences in the radial σ_g profiles, the radial profiles

[1] If we were to have expressed ν_1 in terms of Ω(2.5 AU), then α would need to be 4 times larger than our nominal values to reproduce the results presented here.

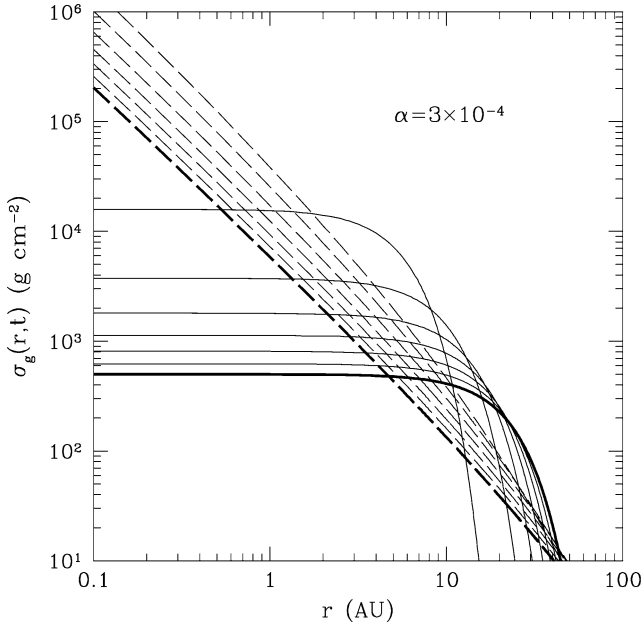

Fig. 1. Surface mass density of the nebula gas, for the two different models we will study in this paper: constant viscosity models (solid lines) and constant αc^2 models (dashed lines). The mass density decreases with time; the curves begin at our first timestep (7×10^4 years), and then are plotted on even multiples of 0.5 Myr until 3 Myr (3 Myr curves are plotted with a heavier weight). This set of evolutions is for nebula $\alpha = 3 \times 10^{-4}$. The case 2 viscosity is multiplied by a factor of 3 to keep the mass fluxes of the two models (Fig. 2) in good agreement at each timestep.

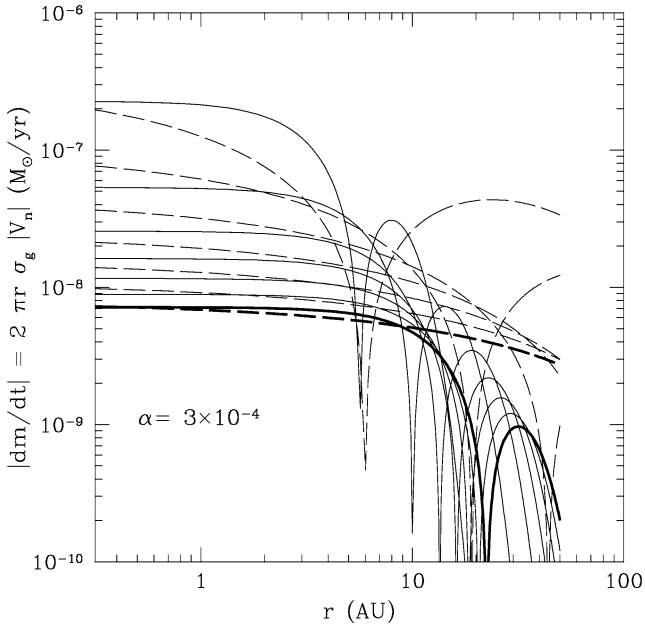

Fig. 2. Radial mass flux of material (absolute value) as a function of radius and time, for the two models of Fig. 1. The mass flux decreases with time; values are plotted at the initial timestep (7×10^4 years) and then every 0.5 Myr from 0.5 until 3 Myr (heavy curves at 3 Myr). Inwards of the cusp, mass flux is inwards (negative); outwards of the cusp, the mass flux is positive (outwards). The mass fluxes for the two cases are aligned by a factor of 3 increase in the viscosity of the constant αc^2 model relative to $\alpha = 3 \times 10^{-4}$ (Section 2.1).

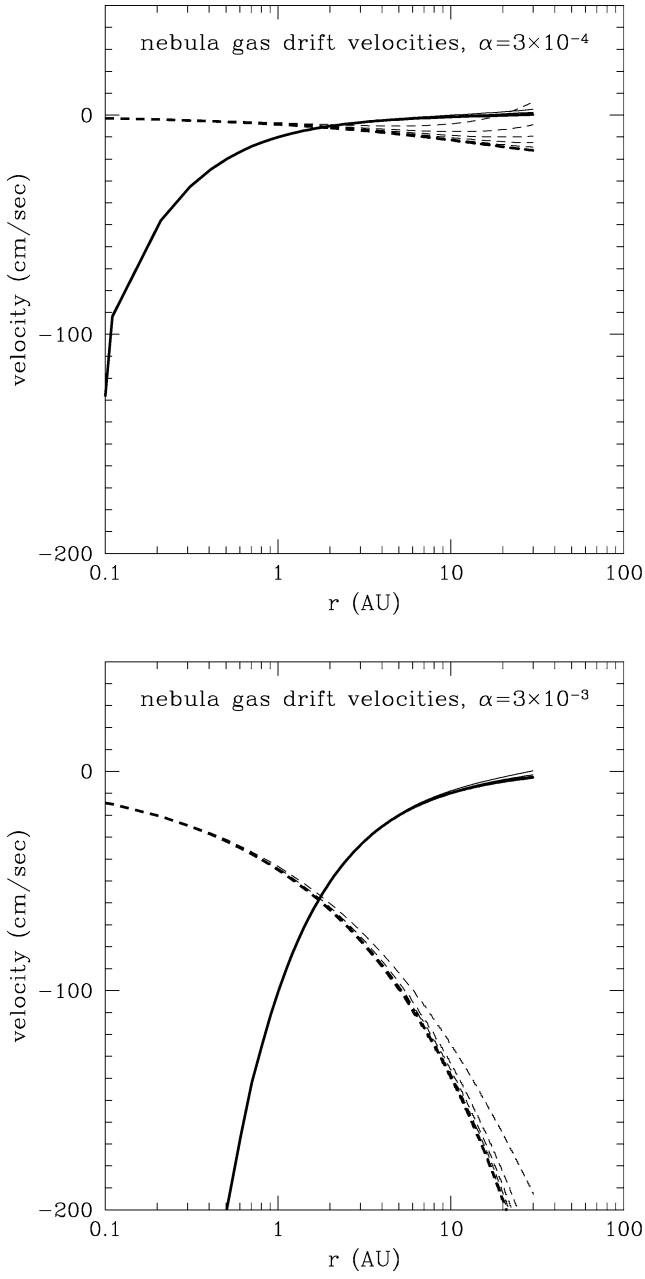

Fig. 3. Nebula gas velocities as functions of radius and time, for the two viscosity models (solid: constant viscosity models; dashed: constant αc^2 models). Upper plot: gas drift velocities for $\alpha = 3 \times 10^{-4}$; lower plot: gas drift velocities for $\alpha = 3 \times 10^{-3}$.

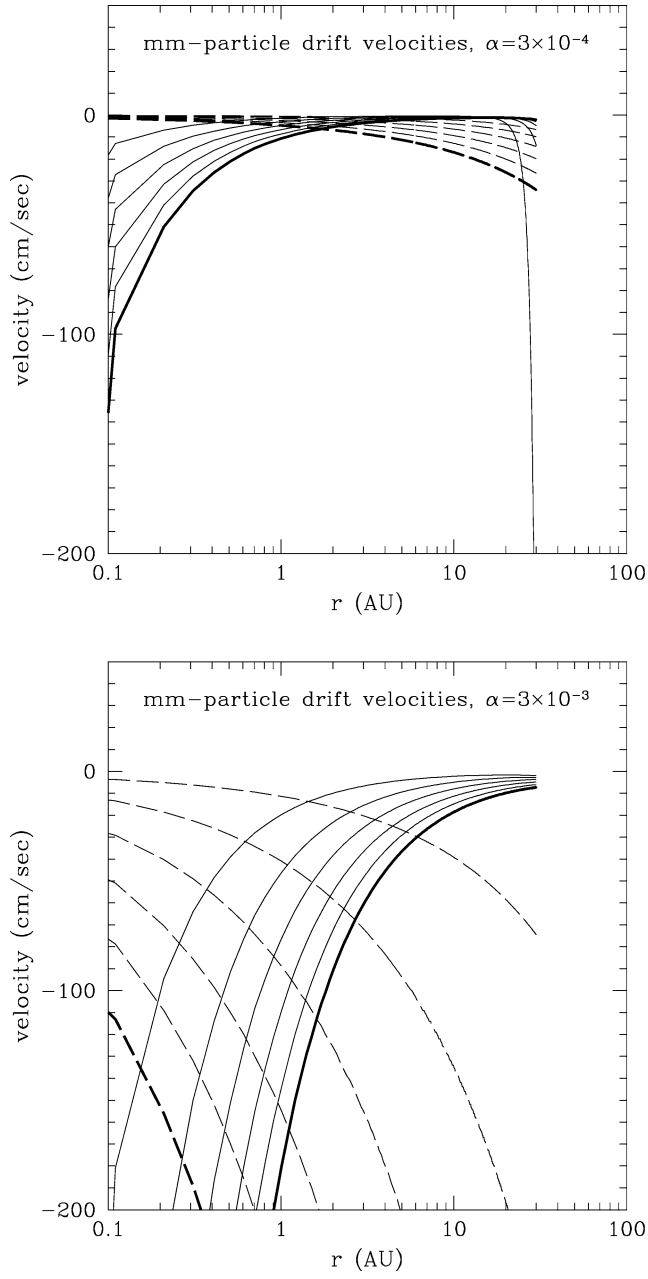

Fig. 4. Millimeter-radius (unit density) particle drift velocities as functions of radius and time, for the two viscosity models (solid: constant viscosity models; dashed: constant αc^2 models). Upper plot: particle drift velocities for $\alpha = 3 \times 10^{-4}$; lower plot: particle drift velocities for $\alpha = 3 \times 10^{-3}$. The larger drift velocities are caused by the fact that the nebula evolves more rapidly at higher α values, and thus the gas density is lower at any given time, resulting in a larger t_s and a larger V_d (see Eq. (2)).

of mass influx are quite similar and are nearly independent of radius in the inner Solar System. The similarity in mass flux profiles (Fig. 2) is related to the different radial velocity profiles (Fig. 3). In fact, it is a natural feature of the LBP solutions that the radial dependencies of σ_g and ν_T nearly cancel throughout the mass inflow region. The nearly constant mass influx depends on their product (cf., e.g., Lin and Papaloizou, 1985). This suggests, for instance, that $\sigma_g(r, t)$ would be proportional to r^{-1} for a viscosity $\nu_T \propto r$ such as suggested by Hartmann et al. (1998) or proportional to $r^{-1/2}$ for the shear-driven β-viscosity profile $\nu_T \propto r^{1/2}$ suggested by Richard and Zahn (1999) (see also Davis, 2002). The mass flux and overall nebula mass decrease with time as expected, with magnitudes (in solar masses per year) which are typical for nebulae of age 10^5–10^6 years (radially outwards of the cusps in Fig. 2, the mass flux reverses and is outwards). The disk mass decreases to a few times $10^{-4} M_\odot$ (case 2) or to a few times $10^{-2} M_\odot$ (case 1) in the 2 Myr timeframe.

Table 1

Parameter	Definition	Value or range
	Model parameters	
$M_\odot$	Stellar mass	2×10^{33} g
M_D	Protoplanetary nebula mass ($t = 0$)	$0.2 M_\odot$
h_o	Solar System specific angular momentum	$9.5 \times 10^{19} \mathrm{cm}^2/\mathrm{sec}$
c	Gas molecule thermal speed	1 km/sec
H	Nebula vertical scale height	$0.05 \times$ radius
α	Turbulent diffusivity parameter	$3 \times 10^{-4} - 3 \times 10^{-3}$
$\mathcal{D}, \nu_T$	Nebula turbulent diffusivity and viscosity	$\alpha c H$
$t_{\max}$	Duration of hot inner nebula CAI source region	10^5 yr
Δt	Code evolutionary timestep $\approx t_c$	5×10^4 yr
r_B	Inner boundary for normal silicates ($t < t_{\max}$)	2.0 AU
r_A	Inner boundary for refractories ($t < t_{\max}$)	0.3 AU
r_i	Inner boundary of nebula	0.01 AU
r_D	Angular momentum or centrifugal radius	4.5 AU
Ω_D	Angular velocity at centrifugal radius	
	Other quantities	
r_p, d_p	Particle radius and diameter	
t_s	Particle stopping time due to gas drag	Eq. (1)
$f_{\mathrm{sil}}, f_{\mathrm{cai}}$	Silicate/hydrogen, CAI/silicate mass fractions	0.005, 0.05
C, C_o	CAI material concentration in general, and nominal	Eq. (14)
E	Enhancement of CAI concentration relative to nominal	Eq. (17)
St	Particle Stokes number	Eq. (1ff)
V_d, V_{dB}	CAI particle radial drift velocity in general and at r_B	Eqs. (2), (3)
V_n, V_{nB}	Nebula radial evolution velocity in general and at r_B	Eqs. (2), (3)
V_K, Ω	Keplerian velocity and orbit frequency	
V_L, V_{LB}	Large particle drift velocity in general and at r_B	
γ	Pressure gradient term affecting gas drag	Eq. (2)
$\sigma, \sigma_1, \sigma_2, \sigma_g, \sigma_{gB}$	Nebula gas surface densities	Eqs. (6), (8)
σ_L, σ_{LB}	Large particle surface density in general and at r_B	
$\mathcal{F}_1, \mathcal{F}_2$	Parameters determining enhancement E of C	Eqs. (18), (19)

2.2. The CAI factory

For the purpose of this modeling exercise, we adopt a highly simplified picture of the environment in which CAIs may have formed and evolved. Such a simplified model can only be asked to address the crudest possible characterization of the CAIs themselves. CAIs are primarily oxides and silicates of calcium, aluminum, and magnesium, with small amounts of titanium and other refractory elements (MacPherson et al., 1989; Brearley and Jones, 2000). Some CAIs appear to be, essentially, *condensates* or aggregates of condensates from a cooling high temperature gas, chemically modified to greater or lesser degree by subsequent *reaction* with the surrounding gas as it continues to cool, and/or subsequent but limited duration *heating events* (e.g., MacPherson and Davis, 1994, especially their Fig. 11). Other kinds of CAIs are "*igneous*" in that they seem to have solidified from a melt—possibly a melt of earlier condensates (e.g., MacPherson et al., 1989; Grossman et al., 2002). The most *widely occurring* type of CAIs (type A), which are found in essentially all meteorite classes, are the smallest, contain the highest temperature minerals, and have the closest structural appearance to simple condensates; the most *abundant* (type B) CAIs, which are found almost entirely in one (CV) chondrite class, are larger, tend to be more dominated by lower temperature (but still relatively refractory, low-Silicon) minerals, and tend more to manifest recrystallization from a melt than condensation from a gas.[2]

The condensation–reaction process has not continued to completion in either case (G. MacPherson, personal communication, 2002), arguing against a simplistic formation process in which CAIs are always in equilibrium with the same parcel of gas as it cools over infinite time. It will ultimately be necessary to relate timescales of nebula radial evolution (outwards, into cooler regions) to timescales of chemical equilibration of the object with the surrounding gas. Our model offers the potential for quantitative assessments of this type.

While complications are easy to imagine (multiple, relatively brief heating events, vertical thermal structure, and so on), we present a simple picture based on prior models of inner nebula energetics and temperature as an initial context for pondering these two very different refractory particle types. Our simple picture (Fig. 5) is that the innermost nebula is sufficiently hot at early times out to some

[2] Rigorously, "type A" and "type B" refer to specific mineralogies, traditionally those found in CV chondrites, as well as to their characteristic size, porosity, and petrography. Here we will suppress some of the mineralogical fine points, considering type A's as small, porous, unmelted condensates, and type B's as large, less refractory, and melted since condensation.

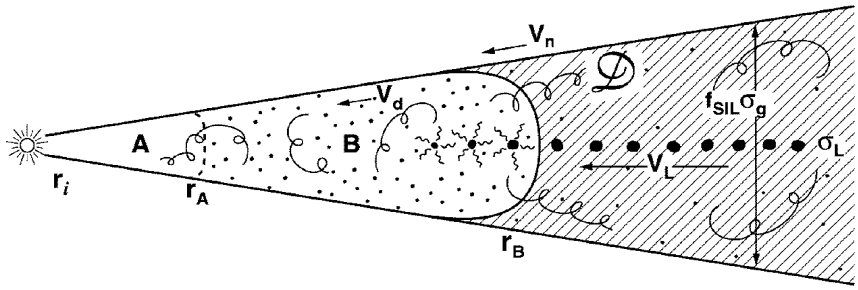

Fig. 5. Cartoon of the hot inner nebula region we adopt for this paper. Region A, between r_i and r_A, is hot enough to evaporate all silicates and refractory oxides. Region B, between r_A and r_B, is hot enough to evaporate all ferromagnesian silicates and metals, but will allow refractory oxides to remain solid. Nebula models indicate $r_A \sim 0.2$ AU and $r_B \sim 2$ AU in the 10^5 year timeframe, and decrease quickly afterwards. The nebula evolves inwards at V_n, CAIs drift relative to the gas at V_d, and meter-sized particles, with surface mass density σ_L, drift at the larger speed V_L. The gas has surface mass density σ_g and is turbulent, with diffusion coefficient $\mathcal{D}$. Silicate "dust" represents $f_{\rm sil}$ of the total disk mass density.

boundary r_A for *all* silicates and refractory oxides (CAIs) to evaporate. Beyond that radius, to some other radius r_B, CAI minerals can exist as solids, but normal ferromagnesian silicates (chondrules and matrix) cannot. In this region the temperature is nearly constant—buffered by condensation of ferromagnesian silicates at the coolest vertical levels (Bell et al., 1997; Cassen, 2001). As the nebula cools, the radial boundaries of these regions sweep inwards. While many earlier models seemed to indicate that the inner nebula was never hot enough to evaporate silicates (see discussion in Wood and Morfill, 1989), more recent models seem to allow this. For instance, model calculations by Ruden and Pollack (1991), Bell et al. (1997), Stepinski (1998), and Cassen (1996, 2001) indicate that $r_A \sim 0.3$ AU and $r_B \sim 2$–3 AU at 10^4 years, decreasing to $r_A \sim 0.01$ AU and $r_B \sim 0.3$ AU by 10^5 years or so. Midplane temperatures at 1 AU derived by Woolum and Cassen (1999) for a number of T Tauri stars approach values adequate to evaporate silicates, for systems with $\dot{M} > 10^{-7} M_\odot$/yr. Note especially that Bell et al. (1997) show that temperatures are higher for lower α values, at any given mass influx rate. The very fact that the vast bulk of meteoritic materials are isotopically *normal* to a very high degree suggests initial vaporization of a significant fraction of their precursors (e.g., Kerridge, 1993). We will adopt these constraints in our model of the CAI source region. Formation of all CAIs only very near to the Sun (e.g., Shu et al., 1996) would restrict the source to something like 0.1 AU or less. In our model calculations, we will treat two idealized particle size ranges: "type A," or < 1 mm diameter objects and "type B," or > 5 mm diameter objects—while larger examples of both CAI types are known to exist in smaller numbers. We tentatively associate "type A" condensates with source region A and "type B" igneous CAIs with source region B.

2.2.1. Enhancement of silicates and carbon in the source regions

A new aspect of the model we advance here is a large enhancement in silicate abundance in the inner Solar System resulting from evaporation of rapidly drifting meter-sized agglomerates of very primitive solid material (which accreted further out, at lower temperatures). This short-circuit for transporting silicate material into the inner Solar System determines the local mass fraction of vapor in region A from which CAIs eventually form, and/or the abundance of unvaporized CAIs in region B (both relative to nebula hydrogen). This drift-based enhancement process has a limited duration—once the inner nebula cools below the evaporation temperature of silicates, drifting meter-sized particles *are* lost directly into the Sun. Thus, this enhancement has a natural association with the early formation ages associated with CAIs.

The subject of the accumulation of macroscopic particles and planetesimals is a very complicated one, and a full description of this process is beyond the scope of this paper. The reader is referred to Weidenschilling (1989, 1997, 2000, 2002), and Weidenschilling and Cuzzi (1993), for descriptions and some typical recent results. While specific results are highly dependent on model assumptions, some generalizations can be attempted.

For the purpose of this paper, we draw the following generalizations from previous studies:

(1) The formation of meter-sized particles is relatively easy (in $\sim 10^3$–10^4 years at several AU) in either turbulent or non-turbulent nebulae, but growth beyond meter size can be severely hindered in turbulent environments. For instance, Eq. 12ff of Weidenschilling (1989) leads to a maximum particle radius of ~ 100 cm for $\alpha = 10^{-4}$, by substituting $V_t = V_g = c\alpha^{1/2}$ (the disruption strength is, of course, quite uncertain). In fact, since planetesimals form rapidly in current (nonturbulent) models (e.g., Weidenschilling, 2000), some level of turbulence might be *required* merely to delay the process by the 10^6 year times observed.
(2) For weak but finite nebula turbulence such as we assume, the radial drift velocity of meter-sized particles is not decreased by collective effects because the midplane density is never large.
(3) The particle size distribution for meter-and-smaller size particles can be approximated by a powerlaw of the form $dN(r) = r^{-3} d(\log r)$; this implies roughly equal

mass per logarithmic radius interval up to meter-sized particles—that is, over 5–7 decades of particle size.[3] Based on the width and form of the rubble particle size distribution mentioned above, we estimate that during the early CAI-forming stage, meter-sized particles represent approximately 10% of the local mass density wherever silicates can be solid.

Drifting meter-sized silicate agglomerates, rather than being "lost into the Sun" during this stage, evaporate as they traverse these inner hot regions. To estimate how much mass is lost by evaporation, we calculated the evaporation rate of pure forsterite using vapor pressure curves of Mysen and Kushiro (1988) and Nagahara et al. (1994), and expressions from Supulver and Lin (2000) and Lichtenegger and Komlë (1991). The evaporation time of a meter-radius boulder in our nominal nebula (at pressure of about 1 mbar) varies from 4600 years at 1550 K to 50 years at 1700 K (see also Fig. 10 of Nagahara and Ozawa, 1996). The time for such a boulder to drift into the Sun from $r_B = 1$ AU is about 100 years. The drifting particles have a collisional lifetime that is less than this, and their fragments will drift more slowly while evaporating more quickly. Also, forsterite is the most refractory ferromagnesian silicate, so realistic material will evaporate faster. For the purpose of this paper we assume the drifting boulders all evaporate and their constituent vapors are homogenized in regions A and B. More detailed calculations of how the silicate vapor source function varies with radius might be appropriate for incorporation in a more detailed numerical model.

Because the inward loss rate of vaporized silicate material due to nebula viscous evolution into the Sun is so much smaller then the arrival rate in large particles, mass conservation causes a large enhancement relative to solar abundance of silicate-forming material in either the vapor phase, or as small residual refractory objects. This is the radial analog of a scheme advocated by Cassen (2001) in which vertical sedimentation played a similar role in enhancing heavy element abundance. A similar effect was discussed by Supulver and Lin (2000) and Cyr et al. (1998) for drifting water ice particles at a larger radial distance. Below we present a toy model which assesses the significance of this process for the CAI factory.

Consider the hot inner Solar System as sketched in Fig. 5. The region between r_B and r_A is hot enough (> 1300 K) to evaporate ferromagnesian silicates (95% of rock-forming materials; Larimer, 1989), but not refractory silicates or oxides—which survive as particulates or, perhaps, molten droplets under certain conditions. Silicates enter the region at r_B. Primordial material (e.g., heterogeneous, cometary-like, perhaps even interstellar-like IDPs) making its way into this region for the first time probably contains no CAI minerals as such, so, as discussed above, we assume that all silicates evaporate on their first pass through region B. However, because region B is simultaneously cool enough for refractories to condense, a haze of fine CAI-type mineral grains might perhaps appear quickly, and without regard for the standard condensation sequence (J. Paque, personal communication, 2002). This population might be related to "fine-grained" CAIs, and of course would also be subject to subsequent melting processes of as-yet unknown nature. The innermost nebula between r_i and r_A is hot enough (1900 K) to evaporate everything which reaches it. Vaporized material drains into the Sun at r_i, along with the nebula hydrogen. At values of $\mathcal{D}$ characterizing our models, we can assume that the concentration C of refractory material (relative to the gas)—whether small solid particles or vapor—is quickly homogenized throughout the relatively narrow regions A and B.

We obtain the CAI material concentration C, as a mass fraction relative to nebula hydrogen, by solving a simple "leaky barrel" mass balance equation for regions A and B as a unit, with both "large" (m-sized) and small particles entering at r_B, small particles and vapor diffusing outwards from the region at r_B, and vapor draining into the Sun at r_i.

$$\frac{d}{dt}\left(2\pi r\overline{\sigma_g(r,t)}\Delta r C\right) = \frac{dm^+}{dt} - \frac{dm^-}{dt}, \tag{10}$$

where

$$\frac{dm^+}{dt} = 2\pi r_B\left(C_o\sigma_{gB}(V_{nB}+V_{dB}) + f_{\rm cai}\sigma_L V_{LB}\right), \tag{11}$$

$$\frac{dm^-}{dt} = 2\pi\left(r_i C\sigma_{gi}V_{ni} + r_B\mathcal{D}\sigma_{gB}\left|\frac{dC}{dr}\right|\right). \tag{12}$$

In these equations, $\sigma_g, \sigma_L, V_n, V_d$, and V_L are surface gas and large particle mass densities, nebula inward evolution velocity, and mm-sized and large particle drift velocity, respectively. The overline indicates a spatial average over the source region of width Δr. $C_o \equiv f_{\rm cai} f_{\rm sil}$ is the nominal, solar abundance of refractory-forming materials by mass relative to hydrogen. This equation may be rewritten as

$$\frac{\overline{r\sigma_g(r,t)}\Delta r}{r_B\sigma_{gB}(V_{nB}+V_{dB})C_o}\frac{dC}{dt} = \left(1 + \frac{f_{\rm cai}\sigma_L V_{LB}}{C_o\sigma_{gB}(V_{nB}+V_{dB})}\right) - C\left(\frac{r_i\sigma_{gi}V_{ni} + \mathcal{D}\sigma_{gB}(r_B/\lambda)}{C_o r_B\sigma_{gB}(V_{nB}+V_{dB})}\right). \tag{13}$$

We have simplified the diffusion term of the above equation by taking $dC/dr \sim C/\lambda$, where λ is the (variable) radial gradient scale due to diffusion itself, and assuming $C \gg C_o$ (which will be verified).

To solve this equation we first define a dimensionless timescale $t' = t/t_c$, where

$$t_c = \frac{\overline{r\sigma_g(r,t)}}{r_B\sigma_{gB}}\frac{\Delta r}{(V_{nB}+V_{dB})}. \tag{14}$$

[3] The particular powerlaw seen in Weidenschilling's various model results might be partly the result of a model assumption regarding ejecta size distributions, and the relative fraction of meter-sized particles could be higher or lower. However, preliminary unpublished results by J.N.C. and Dr. P. Estrada suggest that powerlaws of this sort are self-similar and self-sustaining, and thus perhaps fairly general.

In the above expression for t_c, the ratio $(\overline{r\sigma_g(r,t)}/r_B\sigma_{gB})$ is a factor of order unity which depends on the nebula model, and we neglect it here as a first treatment. Then from Fig. 3 we estimate $t_c \approx (1-5)\times 10^4$ years. t_c may be thought of as the time in which normal evolutionary drift replenishes, or removes, material in a region of width Δr.

Secondly, in the radial range of interest, the inward mass flux $2\pi r\sigma_g V_n$ is essentially independent of radius (Fig. 2), leading to cancellations in the last term of Eq. (13) (to order unity). Then, with the further definition of $C' = C/C_o$, Eq. (13) simplifies to

$$\frac{dC'}{dt'} = (1+\mathcal{F}_1) - C'(1+\mathcal{F}_2) \tag{15}$$

which has the simple solution

$$C' = E - (E-1)e^{-(1+\mathcal{F}_2)t'}. \tag{16}$$

In the equations above,

$$E = \left(\frac{1+\mathcal{F}_1}{1+\mathcal{F}_2}\right), \tag{17}$$

$$\mathcal{F}_1 = \frac{f_{\rm cai}\sigma_L V_{LB}}{C_o\sigma_{gB}(V_{nB}+V_{dB})}, \tag{18}$$

$$\mathcal{F}_2 = \frac{\mathcal{D}\sigma_{gB}(r_B/\lambda)}{\sigma_{gB}(V_{nB}+V_{dB})r_B} \approx \frac{\mathcal{D}}{\lambda V_{nB}} \approx \frac{r_B}{\lambda}. \tag{19}$$

The enhancement E increases as time proceeds and λ increases, but approaches a limiting value on the timescale $t_c/(1+\mathcal{F}_2)$. The term $\mathcal{F}_1$ is the ratio of mass inflow due to large particle drift, to that due to gas advection of grains. The term $\mathcal{F}_2$ is the ratio of outward diffusive mass flux to inward advective flux. First consider the term $\mathcal{F}_2 \sim r_B/\lambda$. Inspection of the Green's functions in Fig. 6 (next section) indicates that λ very quickly approaches r_B, so on the timescale t_c, $\mathcal{F}_2 \sim 1$ and $E \approx (1+\mathcal{F}_1)/2$.

If the drifting large particles were to contribute negligibly to the inward mass flux, $\mathcal{F}_1 \ll 1$ and $C \approx C_o \approx f_{\rm cai} f_{\rm sil}$ for CAIs, where $f_{\rm sil} \approx 0.005$ is the silicate fraction relative to the gas and $f_{\rm cai} \approx 0.05$ is the canonical fraction of silicates which are refractory (Larimer, 1989). However, estimates indicate that the drifting large particles in fact dominate the inward mass flux of solids. The ratio $f_{\rm cai}\sigma_L/C_o\sigma_{gB} = \sigma_L/f_{\rm sil}\sigma_{gB}$ is the mass fraction of solids residing in meter sized particles, which we argued earlier in this section is plausibly on the order of 10^{-1} for particle size distributions such as derived by Weidenschilling (1997, 2000, 2002), if growth beyond meter-size is hindered by energetic collisions in turbulence. A generally expressed estimate of E can be derived as follows, assuming $V_{db} \approx V_{nB}$ at r_B (Figs. 3 and 4) and using Eq. (3) for V_{nB}:

$$E \approx \frac{\mathcal{F}_1}{2} = \frac{f_{\rm cai}\sigma_L}{4C_o\sigma_{gB}}\frac{V_{LB}}{V_{nB}} \approx \frac{f_{\rm cai}\sigma_L}{4C_o\sigma_{gB}}\frac{V_{LB}r_B}{\mathcal{D}}$$
$$\approx 10^{-1}\frac{\gamma V_K r_B}{4\alpha c H} \approx 10^{-1}\frac{\gamma}{4\alpha}\left(\frac{r_B}{H}\right)^2 \approx 10\frac{\gamma}{\alpha}. \tag{20}$$

For $\gamma = 2\times 10^{-3}$ and $\alpha \sim 3\times 10^{-4}$–$3\times 10^{-3}$, as explored in this paper, $E \sim 10$–100. This simple estimate is surely uncertain at the factor of several level. It is interesting that a silicate-to-hydrogen enhancement factor in this range has been inferred for CAI formation from detailed chemical and mineralogical modeling by Alexander (2003).

2.2.2. The role of carbon: chemical and isotopic properties of the CAI factory

We again note, qualitatively, how the fact that the drifting material is millions of years younger, less processed, and far more primitive than "chondritic" can help explain some of the chemical and isotopic properties of CAIs and other early, high-temperature condensates. The material is in all likelihood enriched in carbon by an order of magnitude over CI (Jessberger et al., 1988; Jessberger and Kissel, 1991; Lawler and Brownlee, 1992), and a significant amount of it is in phases which remain solid to high temperatures (Wooden, 2002; Fomenkova, 1997). Instead of increasing the nebula oxygen fugacity as silicates evaporate, much of the silicate-related oxygen could combine with the carbon to produce CO and CO_2, in relative abundance perhaps 1000 : 1 (Lodders and Fegley, 2002; see their Figs. 6 and 10, for enhanced Fe/H). This may help explain two different aspects of CAI formation at the same time.

The first effect is chemical: a carbon sink for oxygen (Connolly et al., 1994) may help explain how CAIs can form in a gas of nearly solar oxygen fugacity (Beckett et al., 1988) even after evaporation of all this silicate material. The second effect is isotopic. There are now several indications that the tendency of CAIs and other early condensates to be enriched in ^{16}O relative to all other solid objects, in a mass-independent fashion, reflects their condensation from an ^{16}O-enriched gas, rather than from ^{16}O-rich solid precursors (Nittler et al., 1997; Hiyagon and Hashimoto, 1999; Krot et al., 2002). Several ways of increasing the ^{16}O content of the gas from which CAIs condense, in the presence of symmetric molecules such as CO_2, were reviewed by Thiemens (1996, 1999). The asymmetry provided by incorporation of the heavy isotopes ^{17}O and ^{18}O into excited state CO_2 or CO_3 allows them to radiate away their energy faster and remain bound more frequently, thus preferentially removing ^{17}O and ^{18}O from reactive states in the gas and leaving the gas enriched in ^{16}O (see also Gao and Marcus, 2001). A concern with this scenario is whether its mass-independence will be preserved at the high temperatures of the hot inner nebula (J. Wasson, personal communication, 2003). Alternate theories exist which operate by elevating the heavy oxygen abundance of the rest of Solar System solids relative to CAIs (Clayton, 2002; Lyons and Young, 2003; Young and Lyons, 2003); however, this perspective must still cope with the apparent absense of appropriately ^{16}O-rich solid precursors (Nittler et al., 1997).

We note that this entire set of environmental conditions—enrichment in silicate vapor, but with solar oxygen fugacity and available CO_2 (and perhaps CO) to affect the isotopic

balance—is due to evaporation of drifting primitive material. The lifetime of this environment is limited by the cooling of the inner nebula below the evaporation temperature of ferromagnesian silicates and refractory carbon, which happens in the first 10^5 years of the life of the nebula. These conditions are thus only associated with the formation age and environment of CAIs and other old, high-temperature condensates.

Summarizing Section 2.2, the CAI source regions could be some combination of an annulus at the condensation temperature of these minerals, which is some fraction of the width of the inner evaporated zone (region A), and a wider, cooler region (region B) where CAI minerals are all that remain of evaporated, meter-sized, silicate particles which drift into the region from their accretion regions farther out. The boundaries of both zones move inwards with time as the nebula cools over perhaps 10^5 years. These source regions, in which CAIs are either produced or "refined," have elevated fractional abundances of CAI material: $C/C_o \gg 1$. In a general way, we will explore the hypothesis that "type A" CAIs are formed (by condensation) in source region A, and that "type B" CAIs are melted and modified in source region B.

2.3. Radial diffusion in the nebula

We use a semi-analytical approach which is simpler, and more amenable to assessing wide ranges of parameter space, than a full numerical solution to the coupled viscous evolution and diffusion difference equations. Clearly, more detailed numerical models would be desirable. Our approach makes use of Green's functions $G(r, r_o; \Delta t)$.[4] The Green's functions we use are the formal solutions to the radial diffusion equation in 2D cylindrical geometry, assuming an instantaneous, narrow cylindrical source of width $\Delta r \ll r_o$ at some radius r_o. They give the resultant diffusion profile at all radii r after some timestep Δt. We use a Δt which is short compared to the nebula evolution time, but much longer than would be required for numerical iteration solutions (Table 1). It is important to note that the quantity which diffuses is the local *concentration* C and not the local *mass density* $C\sigma_g(r,t)$ of CAIs and their vapor precursors; the equation we solve, and to which the Green's functions apply, is (Stevenson, 1990; Bockelèe-Moravan et al., 2002).

$$\frac{dC}{dt} = \frac{1}{\sigma_g r}\frac{\partial}{\partial r}\left(r\sigma_g \mathcal{D}\frac{\partial C}{\partial r}\right) + S_o, \tag{21}$$

where dC/dt is the substantial derivative, and S_o is the source term. We use a timestep which is short relative to the nebula evolution time, because we also need to iterate radial drift of the particles in each timestep. The scheme is as follows:

(1) obtain nebula properties ($\sigma_g(r,t)$ and $V_n(r,t)$) using the LBP solutions;
(2) add the CAI source function S_o, if active, to the local CAI concentration $C(r,t)$;
(3) convolve with the appropriate Green's function to calculate the diffused CAI distribution at time $t + \Delta t$;
(4) calculate the particle drifts relative to the gas over time Δt, and shift particle mass densities (and thus concentrations) accordingly;
(5) use the gas radial drift velocities to shift CAI concentrations radially; and
(6) repeat at next timestep.

In spirit, this is similar to the operator-splitting approach of Bockelèe-Moravan et al. (2002). We assume that the source S_o is only active for 10^5 years, approximately the time it takes the inner nebula to cool below the condensation temperature of silicates. We selected our code timestep of $\Delta t = 5 \times 10^4$ years at the upper end of the range of t_c (the viscous replenishment time of an annulus of width Δr; Eq. (14)). Selecting the smaller end of the range of t_c would produce larger CAI concentrations.

The form of the Green's function will depend on the radial dependence of the diffusivity $\mathcal{D}$. Carslaw and Jaeger (1948, pp. 108–109) derived a Green's function under the condition of radially constant diffusivity:[5]

$$G_1(r, r_o; \Delta t) = 2\pi r_o \frac{e^{-(r^2+r_o^2)/(4\mathcal{D}\Delta t)}}{4\pi\mathcal{D}\Delta t} I_o\left(\frac{r r_o}{2\mathcal{D}\Delta t}\right), \tag{22}$$

where I_o is the modified Bessel function of zero order. The argument of I_o is normally quite large in this application, and numerical difficulties arise in the Bessel function itself. These are avoided by making use of the large argument form $I_o(x) \approx e^x/\sqrt{2\pi x}$, which is adequate over the parameter range of interest, to combine offsetting terms and rewrite the Green's function as:

$$G_1(r, r_o; \Delta t) \approx \sqrt{\frac{r_o/r}{4\pi\mathcal{D}\Delta t}}\, e^{-(r-r_o)^2/(4\mathcal{D}\Delta t)}. \tag{23}$$

Equation (23) above is similar to the more familiar 1D cartesian version, except for a factor accounting for the cylindrical geometry. In our numerical models we use the exact small argument form of I_o when appropriate.

For the constant αc^2 case, in which viscosity ν_T varies as $r^{3/2}$, we needed to derive a different form of the diffusion solution, one which assumes the proper radial variation of the diffusivity. This turns out to be

$$G_2(r, r_o; \Delta t) = 2\pi r_o \left(\frac{r_D^2}{r r_o}\right)^{3/4} \frac{e^{-4r_D^{3/2}(r^{1/2}+r_o^{1/2})/\mathcal{D}_D t}}{\pi\mathcal{D}_D t} \times I_3\left(\frac{8 r^{1/4} r_o^{1/4} r_D^{3/2}}{\mathcal{D}_D t}\right), \tag{24}$$

[4] After submission, we learned that a similar approach had been pursued, and consistent results obtained, by Clarke and Pringle (1988).

[5] We have rewritten the source "strength" Q of Carslaw and Jaeger in terms of a source concentration C_o, as $Q = 2\pi r_o C_o \Delta r$.

where $\mathcal{D}_D$ is the diffusion coefficient or viscosity at r_D, and $I_3(x)$ is the modified Bessel function of third order. The large argument form of G_2 is:

$$G_2(r, r_o; \Delta t) \approx \frac{(r_o/r)^{7/8}(r_D/r_o)^{3/4}}{\sqrt{4\pi\mathcal{D}\Delta t}} \times \exp\left(-\frac{4r^2(1-(r_o/r)^{1/4})^2}{\mathcal{D}(r/r_D)^{3/2}\Delta t}\right). \quad (25)$$

The solution for the diffused concentration at subsequent time $t + \Delta t$ is the convolution of $G(r, r_o; \Delta t)$ with the radial distribution of concentration at time t:

$$C(r, t+\Delta t) = \int_{r_{\min}}^{r_{\max}} \big(C(r_o, t) + S(r_o, t)\big) G(r, r_o; \Delta t)\, dr_o, \quad (26)$$

where $C(r_o, t)$ is the concentration distribution and $S(r_o, t)$ is the source at time t, if any.

Typical Green's functions for viscosity laws used to generate Figs. 1 and 2, for several different timesteps, are shown in Fig. 6. It can be seen that on timescales of 10^4 years, the radial gradient scale approaches r for both viscosity laws, as argued in our discussion of enhancement of the source region (Section 2.2). Application of these Green's functions over a finite radial grid $(r_{\min}, r_{\max})$ leads to some mass loss at each timestep, which we correct for by enforcing mass conservation across the diffusion substep only. Mass is lost only by radial inward drift of the nebula, and the particles in it, into the Sun. As a check on the Green's function approach,

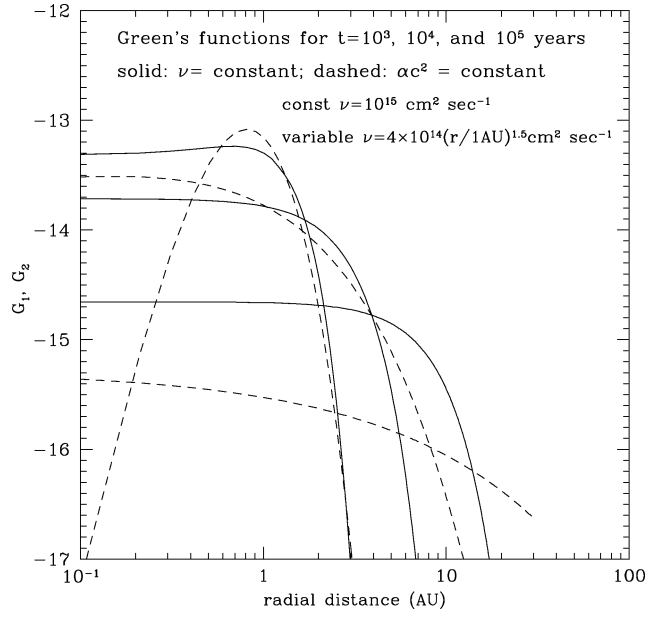

Fig. 6. Sample Green's functions for the two viscosity laws we model (Figs. 1 and 2), with source at $r_o = 1$ AU, for three different timesteps. Solid curves: constant viscosity $\nu_T = 10^{15}$ cm^2/sec (G_1); dashed curves: constant αc^2, or $\nu_T = 4\times10^{14}(r/1\text{ AU})^{3/2}$ cm^2/sec (G_2). The three timesteps are 10^3, 10^4, and 10^5 years, with the shortest timestep corresponding to the narrowest Green's functions.

Taku Takeuchi (personal communication, 2003) kindly ran his model, which solves the diffusion equation using difference equations in the normal way, using a cylindrical delta function for a source term; the results were in good agreement with our Green's function solutions when the same viscosity laws were used.

For this initial exploration of the process, we treat the two potential sources (regions *A* and *B*) separately. The primary difference in the two source types is their radial extent. Region *A* is between 0.01 and 0.3 AU; region *B* is between 1 and 2 AU. Both sources are assumed to be "active" for a duration of 10^5 years.

3. Results

Model calculations of the CAI fractional abundance relative to total silicate abundance are presented in Figs. 7–14. In all cases, the source regions are assumed to be active for 10^5 years. The quantity plotted is the concentration—the fraction of "CAIs" relative to the local abundance of silicates. Volume fractions of CAIs are what is actually observed, but mass fractions are comparable since CAI and chondrule densities are similar. The local abundance of silicates is taken to be a constant fraction $f_{\text{sil}} = 0.005$ of the local nebula gas density as determined by our LBP solutions (Fig. 1, Eqs. (6) and (8)). This simplification neglects the variations in silicate/gas abundance due to the diffusion, drift, and evaporation processes we discuss above (which only operate for a relatively short time and long before primitive body accumulation actually occurs) and decoupling of $\sim 10\%$ of solids in the m-size range. However, future models should account for differential evolution of particles and gas on longer timescales (e.g., Stepinski and Valageas, 1996, 1997; Weidenschilling, 2002).

The figures have a common format: mass fractions obtained from the constant viscosity models are the solid curves; those from the constant αc^2 models, in which viscosity increases as $r^{3/2}$, are the dashed curves. Results are plotted every 0.5 Myr, from 0.5 to 3 Myr. The final curve in each set, at 3 Myr, is shown in a heavier line weight. At the top of each plot is a horizontal bar indicating the radial extent of the main asteroid belt. Results are shown for source regions *A* and *B* separately, for two different particle sizes (diameters of 1 and 5 millimeters, but one case is shown for 10 mm diameter), and two different values of α: 3×10^{-4} and 3×10^{-3}. CAIs with larger sizes than these can be found for both major types; however, some of the larger size CAIs may well be of a lower density because of a high initial porosity, or have a significant irregularity, so would behave aerodynamically like correspondingly smaller particles. Thus we select values close to the mode particle sizes. Different enhancement factors *E* are adopted in the different cases to keep the results in the ballpark of the observations: to wit, large, 5 mm "type *B*" CAIs are found (in CV meteorites) at the 6% level by volume; small, 1 mm "type *A*"

CAIs are found in essentially all meteorite classes at about 1% by volume (Brearley and Jones, 2000; McKeegan et al., 1998; McSween, 1977a, 1977b).[6]

3.1. Small CAIs

We first consider the smaller sized particles, and for these, we first consider the region *A* source. Figures 7 and 8 show results for 1 mm diameter particles, for $\alpha = 3 \times 10^{-4}$ and 3×10^{-3}, respectively. For the $\alpha = 3 \times 10^{-4}$ case, Fig. 7 shows that region *A* is able to supply the observed abundance of small CAIs across the asteroid belt—in fact, well into the outer Solar System—given an enhancement factor in the range of 100–200, depending on viscosity model. This is not an unreasonable value of E for this α (Eq. (20)). This wide dispersal of small particles is compatible with the results of Bockelèe-Moravan et al. (2002). For the constant viscosity model, the volume fraction in small CAIs does not vary strongly with time. Thus, meteorites formed across the asteroid belt and over the entire time period between 1.5–3 Myr might be expected to have the same type and relative abundance of small CAIs. For the constant αc^2 model, the CAI volume fraction decreases more rapidly with time, but a smaller enhancement factor might apply depending on the time between CAI formation and parent body accretion. Here and in all other cases to be discussed, models of intermediate radial dependence of viscosity and surface mass density, naturally, would produce intermediate results.

Figure 8, also for a region *A* source and mm-diameter particles, is for a larger $\alpha = 3 \times 10^{-3}$. The constant viscosity model is marginal here even for the rather generous enhancement factor of 500, which itself is difficult to justify for this value of α given the simple enhancement model we developed (Eq. (20)). The constant αc^2 model does not appear to be a contender for this α.

Consider now the region *B* source, and the same small, mm-diameter particles. Figures 9 and 10 show the results for $\alpha = 3 \times 10^{-4}$ and 3×10^{-3}, respectively. The constant viscosity model can satisfy the observations for either value of α, and with considerably smaller values of E. This is primarily because source region *B* is larger in area than source region *A*. As in the region *A* case, the temporal variation of volume fraction is fairly small for the constant viscosity case, and is larger for the constant αc^2 case. Given the lower enhancements required by a region *B* source, even the constant αc^2 case might be able to hit the mark in the appropriate time window (with a larger enhancement factor).

Concerning the smaller, "type *A*" CAIs overall, while region *B* can satisfy the observations with lower enhancement factors, the plausible physical association of region *A* with a condensation origin of many small CAIs leads us to favor it as the source region for "type *A*" CAIs. Appropriate enhancement factors are somewhat larger than our crude estimates (Eq. (20)) but not implausibly so. However, enhancement factors required for the larger α value ($\alpha = 3 \times 10^{-3}$)

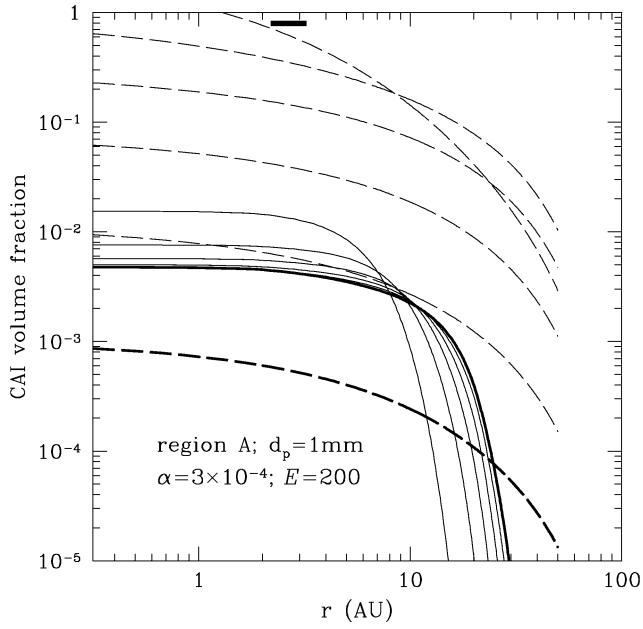

Fig. 7. CAI model concentrations as a function of nebula radius and time, for small CAIs (diameter = 1 mm), and for our two viscosity/surface density models (solid: constant viscosity; dashed: constant αc^2. This figure is for a region *A* source ($r_o < 0.3$ AU), active for 10^5 years. Values are plotted every 0.5 Myr up to 3 Myr (which is plotted with a heavier weight).

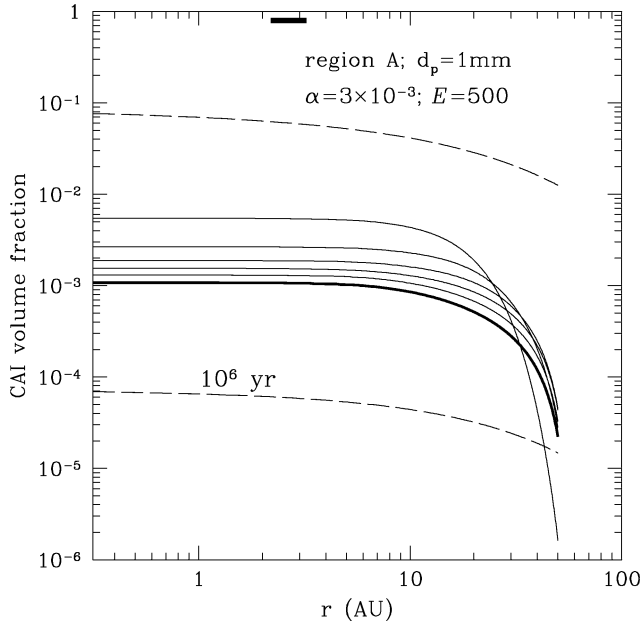

Fig. 8. CAI model concentrations as a function of nebula radius and time, for small CAIs (diameter = 1 mm), and for our two viscosity/surface density models (solid: constant viscosity; dashed: constant αc. This figure is for a region *A* source ($r_o < 0.3$ AU). Values are plotted every 0.5 Myr up to 3 Myr (which is plotted with a heavier weight). An enhancement of 500 is probably unrealistic for this value of $\alpha = 3 \times 10^{-3}$.

[6] Brearley and Jones (2000) tabulate all inclusions (their page 3-190) but McSween distinguishes between true CAIs and other inclusion types, which are less refractory and might have had a longer lasting, or more widespread, "factory" of their own; thus we match only the true CAI abundances.

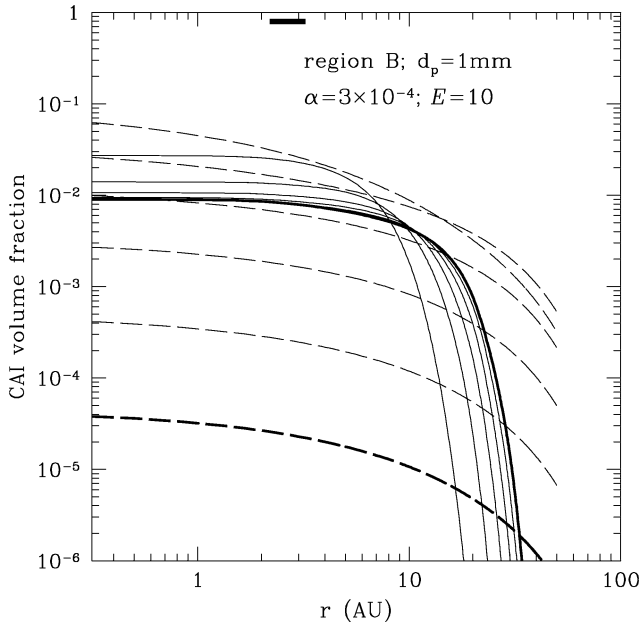

Fig. 9. CAI model concentrations as in Figs. 7 and 8 for small CAIs (diameter = 1 mm). This figure is for a region *B* source ($1 < r_o < 2$ AU). Values are plotted every 0.5 Myr up to 3 Myr (which is plotted with a heavier weight).

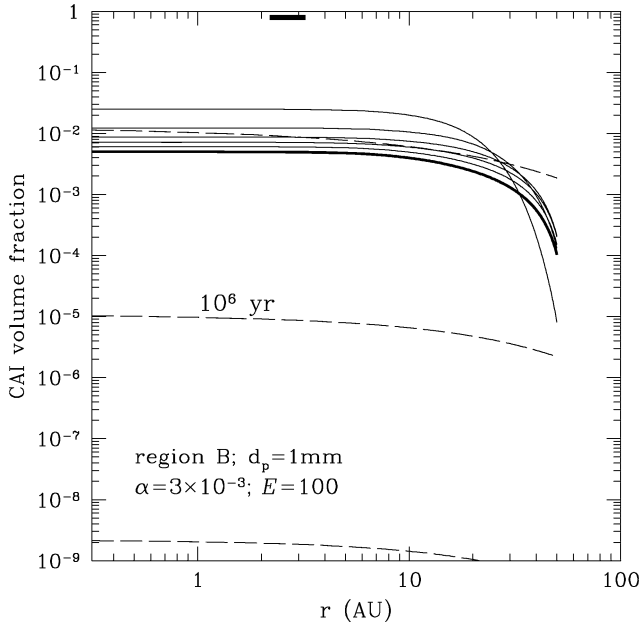

Fig. 10. CAI model concentrations as in Fig. 9, for small CAIs (diameter = 1 mm). This figure is for a region *B* source ($1 < r_o < 2$ AU). Values are plotted every 0.5 Myr up to 3 Myr (which is plotted with a heavier weight).

are not consistent with this α (Eq. (20)), so the lower α is preferred (e.g., Fig. 7). Given that small CAIs are fairly widely seen in similar proportions in all meteorite classes, a situation closer to the constant viscosity model seems to be preferred for either region *A* or *B*.

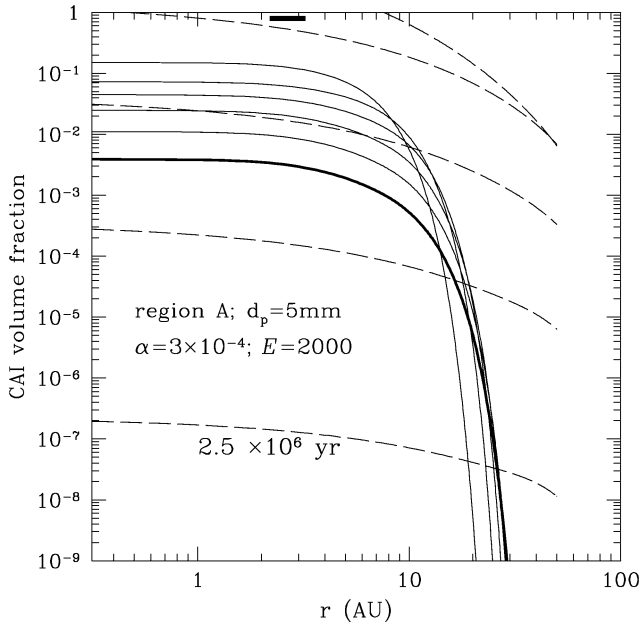

Fig. 11. CAI model concentrations as in Figs. 7 and 8, for large CAIs (diameter = 5 mm). This figure is for a region *A* source ($r_o < 0.3$ AU), and the required enhancement (2000) is probably not plausible.

3.2. Large CAIs

Now we address the larger CAIs, taking them to be of 5 mm diameter typically as representative of the type *B* CAIs which are only seen in one meteorite class (the CV chondrites). The data indicate that these large CAIs constitute around 6% by volume in the CV chondrites (and essentially zero in other classes). Again, we first look at region *A* (0.01–0.3 AU). Figure 11 shows that a region *A* source with $\alpha = 3 \times 10^{-4}$ can only match the observed abundances if the enhancement factor (2000) is well above the maximum plausible value (Eq. (20)). Even for this large enhancement, the steeper nebula viscosity models (dashed lines) are unable to match the observed volume fractions after 1.8 Myr or so. The situation is even worse for the larger α of 3×10^{-3} (Fig. 12), where this large enhancement factor is even less reasonable. Neither viscosity model can retain 5 mm particles for 1 Myr in the observed abundances. So, region *A* is an unlikely source for "type *B*" CAIs within the context of this model.

On the other hand, the region *B* source (1–2 AU) is able to supply the larger particles in the observed abundances because of its larger area and its closer proximity to the asteroid belt. Figure 13, for $\alpha = 3 \times 10^{-4}$, shows that at least the constant viscosity model matches the observations with a plausible enhancement. However, even the region *B* source is questionable if α is as large as 3×10^{-3} (Fig. 14), because for this α an enhancement factor of 1000 is problematic (Eq. (20)) and even then, after 1.5 Myr the model abundances are smaller than the observations of large CAIs require, even for the constant viscosity model.

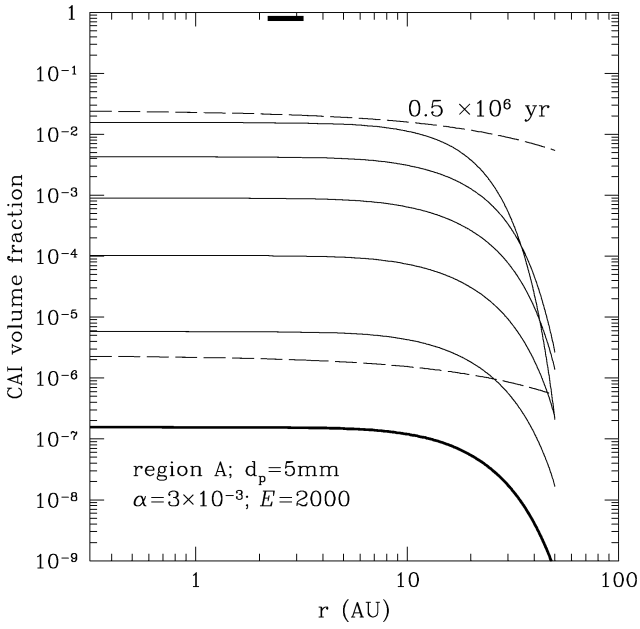

Fig. 12. CAI model concentrations for large CAIs (diameter = 5 mm). This figure is for a region *A* source ($r_o < 0.3$ AU) with $\alpha = 3 \times 10^{-3}$; an enhancement this large would be very hard to justify for this α (Eq. (20)), and even at that, the abundances are significantly lower than observed in the > 1 Myr timeframe.

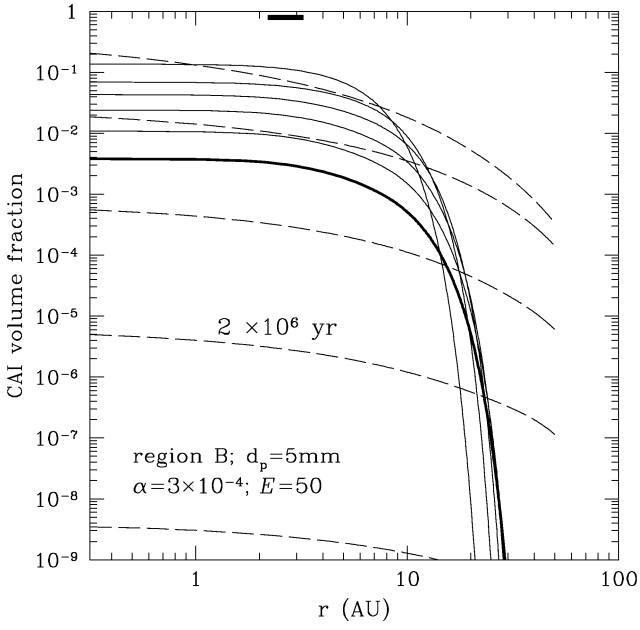

Fig. 13. CAI model concentrations as in Figs. 9 and 10, for large CAIs (diameter = 5 mm). Curves are plotted every 0.5 Myr from 0.5–3 Myr. This figure is for a region *B* source ($1 < r_o < 2$ AU). The observed abundances (6%) may be satisfied by the constant viscosity model with an enhancement factor which is quite reasonable for this α. There may even be enough latitude in E for the steeper viscosity law to satisfy the observations, as well.

Some type *B* CAIs are even larger—in the 1 cm diameter range. Unfortunately, no quantitative data on CAI size distributions exists in the literature to our knowledge. Figure 15 shows results for type *B* CAIs as large as 1 cm in diameter.

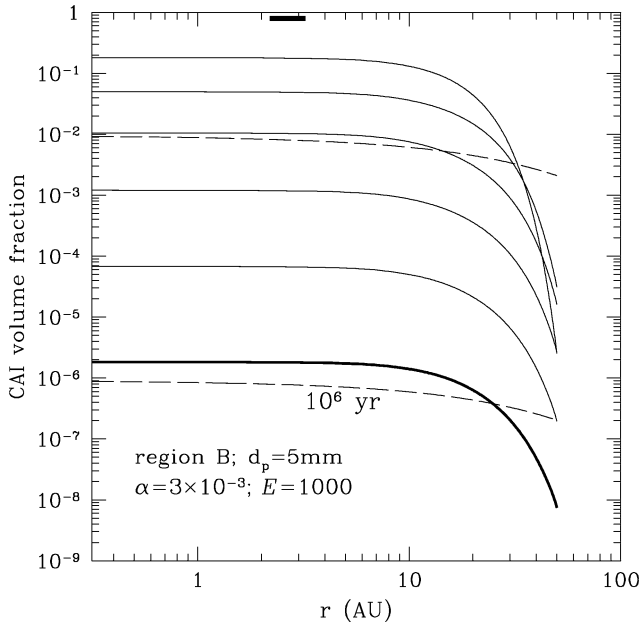

Fig. 14. CAI model concentrations as in Fig. 13, for large CAIs (diameter = 5 mm). This figure is for a region *B* source ($1 < r_o < 2$ AU). For this α, enhancements as large as 1000 are questionable, so neither viscosity law provides a good candidate.

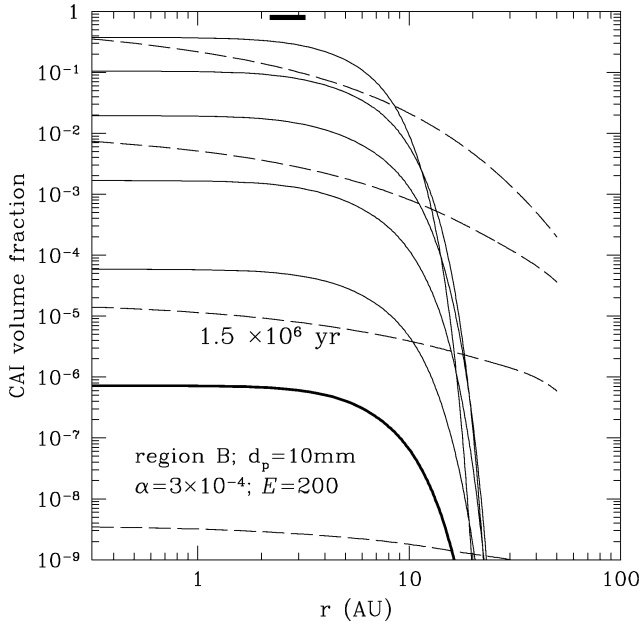

Fig. 15. CAI model concentrations as in previous figures, for especially large CAIs (diameter = 10 mm). This figure is for a region *B* source ($1 < r_o < 2$ AU). There are no quantitative estimates for the fractional abundance of cm-diameter objects.

The larger particles are clearly not so easily retained over periods as long as 3 Myr; however, for a value of E which is not implausible for $\alpha = 3 \times 10^{-4}$, some of these objects can be retained until 1.5–2 Myr or so at least by the constant viscosity model. The abundance decreases even more rapidly than for 5 mm particles, over only a few 10^5 years.

For 5–10 mm diameter CAIs, the time variation of the modeled CAI abundances is much stronger than the radial variation, and because it decreases monotonically with time, a prediction of the model would clearly be that the CV chondrites in which large, "type *B*" CAIs are found should be *accumulated* somewhat *earlier* than other chondrite groups, rather than, say, at the same time but at a different distance from the Sun.

4. Discussion and conclusions

We briefly summarize our results, and mention some additional implications, predictions, and tests of the model.

We have shown that, in a weakly turbulent protoplanetary nebula, outward diffusive mass flux across a concentration gradient can overcome inward mass flux of 1–5 mm diameter particles, by nebula advection and gas-drag-driven radial drift, for times on the order of 10^6 years. The relative abundance of small (1 mm diameter) or highly "fluffy" particles (which behave aerodynamically like smaller, solid particles) is so slowly changing in the 1–3 Myr timeframe that it is not surprising to find them ubiquitously distributed in all meteorite classes. The radial distribution of small objects is fairly uniform, and some redistribution even into the outer Solar System is indicated, consistent with earlier results for even smaller particles by Bockelèe-Moravan et al. (2002). The model thus offers some interesting possibilities for whether or not small CAIs would be observable in comets or IDPs; generally speaking, they would be at lower abundances (sometimes far lower) than in meteorites, but for some parameter choices, they might be present in observable quantities. This result should be treated cautiously, because our model calculates the particle radial drift rate using a constant pressure gradient term γ (see Section 1.2), which will not be the case towards the outer edge of the nebula.

During the very same initial 10^5 years when CAIs seem to have formed, the inner nebula was hot enough to evaporate quite a large mass in inwardly drifting meter-size boulders, thereby greatly enhancing the abundance of silicate material relative to solar. We present a quantitative estimate of the enhancements which might result from this process, and show that plausible enhancements provide quantitative agreement with observed CAI abundances for a range of turbulent viscosities and assumptions as to the radial extent of the source region, as well as with independent estimates based on CAI formation and mineralogy (Alexander, 2003). We suggest that carbon enrichment of these early boulders, relative to CI, might help to explain aspects of meteorite chemistry which argue for solar oxygen fugacity, and for mass-independent fractionation of oxygen isotopes. This silicate-and-carbon enhancement process ceases when the inner nebula cools off—well before chondrules form and primitive bodies accumulate. Thus, the "CAI factory" environment is naturally associated with the early, high temperature condensates which show these properties.

The association of small "type *A*" condensates with source region *A*, and large, "type *B*," igneous CAIs with source region *B*, seems to be plausible. That is, a region *A* (condensation zone) source is able to explain the observed abundance of 1 mm or "fluffy" condensate particles with enhancements in a plausible range. Based on the enhancement factors involved, it seems that only a region *B* source is likely to explain the observed abundances of the larger CAIs. A slightly cooler region *B* is also consistent with the somewhat less refractory mineralogy of type *B* CAIs. Of course, condensate particles from region *A* would need to diffuse outwards through region *B*, allowing those which remain there for a longer time to have the opportunity to coalesce, melt, and/or equilibrate with a somewhat cooler gas. Small "type *A*" condensate CAIs we observe in meteorites today would be those which traversed region *B* quickly, incurring the least processing subsequent to their formation. The larger *E* values associated with region *A* formation of small CAIs might be suggesting that evaporation of drifting rubble culminates primarily at or near the region *A* boundary, rather than uniformly throughout regions *A* and *B*.

5–10 mm diameter particles are retained less easily than 1 mm diameter particles, and their abundance is rapidly decreasing in the 1–3 Myr timeframe. Thus, a prediction and test of the scenario and model presented here is that the CV class of meteorites, which alone contain the large, 5–10 mm CAIs, should have accumulated before the other classes. It is a bit of a puzzle as to why it is said that large CAIs are not only rare, but *nonexistent* in other chondrite classes. Even a drop by an order of magnitude or more should leave some rare occurrences of large CAIs in later-forming classes. This might indicate a layer of complexity not in the current model.

Overall, the viscosities/diffusivities toward the higher end of our range ($\alpha = 3 \times 10^{-3}$) make the scenario less credible, because the high *E* required becomes inconsistent with those very α values. This is because we assume that viscosity evolves the nebula as well as diffusing the particles. Larger α values decrease the nebula gas density more quickly, increasing particle stopping times and inward radial drift speeds faster than outward diffusion can proceed. A model in which the diffusivity and nebula evolution were decoupled might not incur this difficulty, and indeed, turbulent diffusivity is always larger than turbulent viscosity (Prinn, 1990). It should be kept in mind that these α values are normalized at r_D; relating our model *viscosities* to some α at 2 AU would result in α values 4 times *lower*.

4.1. Potential connection with astronomical observations of hot inner disks

Recently, Najita et al. (2003) have found evidence for abundant hot CO emission extending to $\geqslant 1$ AU in T Tauri disks with mass accretion rates in the $\dot{M} = 10^{-9}$—few times

$10^{-7} M_\odot$/yr range. The CO emission increases with $\dot{M}$. Disks with mass fluxes in the $10^{-7} M_\odot$/yr range are in the "early, hot" regime we study in this paper. Najita et al. suggest that the CO emission comes from a temperature inversion high in the disk atmosphere at these radii, possibly caused by X-ray emission from the star. It is interesting to consider how observations of this type may relate to the models considered here. Even though midplane temperatures in these disks are hot enough to evaporate drifting silicates in the 0.2–2 AU region of our models, the photospheres of these disks are likely to be both considerably cooler (100–200 K) and opaque (Woolum and Cassen, 1999). Our model predicts that abundant CO is produced in these regions by evaporation of drifting silicate-carbon rubble; it is not hard to imagine the CO diffusing vertically upwards, right across the photospheric temperature minimum which is not cold enough to freeze it out, and into the tenuous upper disk atmosphere which is heated by stellar X-rays or other processes, where it is seen in emission against the cool, opaque photosphere. As a result of the drift-evaporation-enhancement process discussed here, one might expect the local abundance of CO (relative to hydrogen) to be significantly enhanced over its nominal values. The enhanced silicate vapor simultaneously produced, however, would condense before reaching (and, in fact, create) the disk photosphere, so might not be detectable spectrally. It will be interesting to study these connections further, perhaps making use of other molecules.

4.2. Caveats and future work

The meteorite record is still incompletely sampled, and some specifics of current generalizations may be vulnerable. For instance, Kimura et al. (2002) have observed abundant CAIs in a group of related ordinary (H) chondrites—in spite of the current generalization that CAIs are rare in ordinary chondrites. These appear to be the small, type *A* CAIs which are widely distributed in carbonaceous chondrite classes—but in larger relative abundance than normally found in ordinary chondrites. Moreover, the matrix material in this H chondrite is like that of CO3 chondrites—introducing the possibility that the nature of the fine-grained material, which is expected to diffuse the most intimately with the gas, might be a more important factor in CAI abundance than the chondrule type with which it is mixed. This leaves a diffusive mixing scenario still attractive, but hints at spatial and/or temporal variations beyond the scope of this paper. Clearly, more observations of diverse meteorite types will be enlightening.

Our model is certainly amenable to improvement in many ways. Intermediate, but still analytical, forms of nebula viscosity and mass density distributions can readily be explored with our Green's function approach, but significant improvement beyond that will quickly bring a number of complex parameter variations into play. For instance, a realistic numerical diffusion equation, with coupled accretion and drift, would be required to explore radially and temporally variable viscosity and diffusivity. At the same time, a radially variable pressure gradient term (γ) could be incorporated to address the transport of material to the outer Solar System. In fact, it may be of interest to explore how an extended period when turbulence is extremely low or nonexistent, perhaps after the initial outward diffusion of CAIs has occcurred, might affect the results.

As a large amount of meter-sized material drifts inwards and evaporates, outward and upward diffusion of the vapor precursors of ferromagnesian silicates will occur, with recondensation immediately outside or above the 1300 K boundary region, followed by outward diffusion of the condensate grains. The possibilities for recycling of silicate material through the hot inner zone, including normalization of isotopic ratios for a large mass of inner nebula silicates and meteorite precursors, are intriguing.

A key process which should be explored is the incorporation of a "loss" term into the model (e.g., Cassen, 1996, 2001), whereby grains can be incorporated into much larger particles as they evolve outwards, thereby ceasing their outward evolution and probably settling to the midplane as part of the large particle. Perhaps already solid, mm-to-cm-size CAIs are less efficiently accumulated than vaporized ferromagnesian material, which quickly freezes out into tiny grains or onto the surfaces of already existing grains and particles as the enhanced silicate vapor inside region *B* diffuses outwards across its condensation boundary.

We have not seriously considered the effects of global decoupling of the overall surface mass density of solids from that of the gas on the CAI fraction at the time of planetesimal formation. This could affect the results in either direction. Loss of a substantial meter-sized fraction over several Myr could deplete net solids relative to gas and small particles which are diffusively transported. Ultimately, this process as well as the accretional trapping of CAIs and the recycling of silicate material noted above, needs to be incorporated in a more realistic global model. Other specifics which might affect the global evolution of meter-sized particles, and specifically their radial mass flux, include a growing Jupiter core, vortex trapping, etc.

Finally, realistic timescales for mineralogical and chemical changes by reaction with nebula gas could be combined with this model to assess the timescales on which particles evolve radially through regions of different temperature. This would result in another set of testable predictions. Clearly, there is much work remaining to be done.

Acknowledgments

We are grateful to Gibor Basri, Robbins Bell, Nuria Calvet, John Carr, Pat Cassen, Harold Connolly, Paul Estrada, Tom Greene, Larry Grossman, Lynne Hillenbrand, Sasha Krot, Steve Lubow, Glenn MacPherson, Bjorn Mysen, Katharina Lodders, Mark Marley, Kevin McKeegan, Joan

Najita, Julie Paque, Mark Thiemens, John Wasson, Diane Wooden, and Kevin Zahnle for helpful discussions concerning CAIs, carbon, isotopic fractionation, silicate evaporation, and nebula properties. We thank Robert Last and Robert Hogan for computational and graphics support, Pat Cassen for careful reading of an earlier version and several useful suggestions, and Ignacio Mosqueira and Steve Desch for other helpful comments. We thank Taku Takeuchi for running a numerical test of our Green's function approach. This research was supported by Grants to JNC from the Planetary Geology and Geophysics Program and the Origins of Solar Systems Program. This research has made ample use of the Astrophysics Data System Query and Abstract service.

References

Alexander, C.M.O'D., 2003. Making CAIs and chondrules from CI dust in a canonical nebula. In: Proc. Lunar Planet. Sci. Conf. 34th, March 2003. 1391.pdf (CD-ROM).

Alexander, C.M.O'D., Boss, A.P., Carlson, R.W., 2001. The early evolution of the inner Solar System: a meteoritic perspective. Science 293, 64–68.

Amelin, Y., Krot, A.N., Hutcheon, I.D., Ulyanov, A.A., 2002. Lead isotopic ages of chondrules and calcium–aluminum rich inclusions. Science 297, 1678–1683.

Beckett, J.R., Live, D., Tsay, F.-D., Grossman, L., Stolper, E., 1988. Ti^{3+} in meteoritic and synthetic hibonite. Geochim. Cosmochim. Acta 52, 1479–1495.

Bell, K.R., Cassen, P.M., Klahr, H.H., Henning, Th., 1997. The structure and appearance of protostellar accretion disks: limits on disk flaring. Astrophys. J. 486, 372–387.

Bockelèe-Moravan, D., Gautier, D., Hersant, F., Huré, J.-M., Robert, F., 2002. Turbulent radial mixing in the solar nebula as the source of crystalline silicates in comets. Astron. Astrophys. 384, 1107–1118.

Boss, A.P., 1996. A concise guide to chondrule formation models. In: Hewins, R., Jones, R., Scott, E.R.D. (Eds.), Chondrules and the Protoplanetary Disk. Cambridge Univ. Press, pp. 257–264.

Brearley, A.J., Jones, R.H., 2000. Chondritic meteorites, in "Planetary materials." Rev. Mineral. 36, 191ff.

Carslaw, H.S., Jaeger, J.C., 1948. Operational Methods in Applied Mathematics, 2nd edition. Oxford Univ. Press. Reprinted by Dover, 1963.

Cassen, P., 1996. Models for the fractionation of moderately volatile elements in the solar nebula. Meteorit. Planet. Sci. 31, 793–806.

Cassen, P., 2001. Nebula thermal evolution and the properties of primitive planetary materials. Meteorit. Planet. Sci. 36, 671–700.

Clarke, C.J., Pringle, J.E., 1988. The diffusion of contaminant through an accretion disk. Mon. Not. R. Astron. Soc. 235, 365–373.

Clayton, D., 2002. Self-shielding in the solar nebula. Nature 415, 860–861.

Connolly, H.C., Love, S.G., 1998. The formation of chondrules: petrologic tests of the shock wave model. Science 280, 62–67.

Connolly, H.C., Hewins, R.H., Ash, R.D., Zanda, B., Lofgren, G.E., Bourot-Denise, M., 1994. Carbon and the formation of reduced chondrules. Nature 371, 136–139.

Cuzzi, J.N., Hogan, R.C., 2003. Blowing in the wind. I. Velocities of chondrule-sized particles in a turbulent protoplanetary nebula. Icarus 164, 127–138.

Cuzzi, J.N., Dobrovolskis, A.R., Champney, J.M., 1993. Particle–gas dynamics near the midplane of a protoplanetary nebula. Icarus 106, 102–134.

Cuzzi, J.N., Dobrovolskis, A.R., Hogan, R.C., 1996. Turbulence, chondrules, and planetesimals. In: Hewins, R., Jones, R., Scott, E.R.D. (Eds.), Chondrules and the Protoplanetary Disk. Cambridge Univ. Press, pp. 35–44.

Cuzzi, J.N., Hogan, R.C., Paque, J.M., Dobrovolskis, A.R., 2001. Size-selective concentration of chondrules and other small particles in protoplanetary nebula turbulence. Astrophys. J. 546, 496–508.

Cyr, K.E., Sears, W.D., Lunine, J.I., 1998. Distribution and evolution of water ice in the solar nebula: implications for Solar System body formation. Icarus 135, 537.

Davis, S., 2002. A simplified model for an evolving protoplanetary nebula. Astrophys. J. 592, 1193–1200.

Desch, S., Connolly, H.C., 2002. A model of the thermal processing of particles in solar nebula shocks: application to the cooling rates of chondrules. Meteorit. Planet. Sci. 37, 183–207.

Dubrulle, B., Morfill, G.E., Sterzik, M., 1995. The dust sub-disk in the protoplanetary nebula. Icarus 114, 237–246.

Fleming, T., Stone, J.M., 2003. Local magnetohydrodynamic models of layered accretion disks. Astrophys. J. 585, 908–920.

Fomenkova, M., 1997. Organic components of cometary dust. In: Pendleton, Y., Tielens, A.G.G.M. (Eds.), Stardust to Planetesimals. In: ASP Conf. Ser., Vol. 122, pp. 415–421.

Gail, H.-P., 2001. Radial mixing in protoplanetary accretion disks. I. Stationary disc models with annealing and carbon combustion. Astron. Astrophys. 378, 192–213.

Gao, Q.-Y., Marcus, R.A., 2001. Strange and unconventional isotope effects in ozone formation. Science 293, 259–263.

Grossman, J., 1989. Formation of chondrules. In: Kerridge, J.F., Matthews, M.S. (Eds.), Meteorites and the Early Solar System. Univ. of Arizona Press, pp. 680–696.

Grossman, J., Rubin, A.E., Nagahara, H., King, E.A., 1989. Properties of chondrules. In: Kerridge, J.F., Matthews, M.S. (Eds.), Meteorites and the Early Solar System. Univ. of Arizona Press, pp. 619–659.

Grossman, L., Ebel, D.S., Simon, S.B., 2002. Formation of refractory inclusions by evaporation of condensate precursors. Geochim. Cosmochim. Acta 66, 145–161.

Hartmann, L., Calvert, N., Gullbring, E., D'Alessio, O., 1998. Accretion and the evolution of T Tauri stars. Astrophys. J. 495, 385–400.

Hiyagon, H., Hashimoto, A., 1999. ^{16}O excesses in olivine inclusions in Yamato-86009 and Murchison chondrites and their relation to CAIs. Science 283, 828–831.

Huss, G.R., MacPherson, G.J., Wasserburg, G.J., Russell, S.S., Srinivasan, G., 2001. Aluminum-26 in calcium–aluminum rich inclusions and chondrules from unequilibrated ordinary chondrites. Meteorit. Planet. Sci. 37, 975–997.

Jessberger, E.K., Kissel, J., 1991. Chemical properties of cometary dust and a note on carbon isotopes. In: Newburn Jr., R.L., Neugebauer, M., Rahe, J. (Eds.), Comets in the Post-Halley Era. Kluwer Academic, pp. 1075–1092.

Jessberger, E.K., Christoforidis, A., Kissel, J., 1988. Aspects of the major element composition of Halley's dust. Nature 332, 691–695.

Jones, R.H., Lee, T., Connolly Jr., H.C., Love, S.G., Shang, H., 2000. Formation of chondrules and CAIs: theory vs. observation. In: Mannings, V., Boss, A.P., Russell, S.S. (Eds.), Protostars and Planets IV. Univ. of Arizona Press, p. 927.

Kerridge, J.F., 1993. What can meteorites tell us about nebular conditions and processes during planetesimal accretion? Icarus 106, 135–150.

Kimura, M., Hiyagon, H., Palme, H., Spettel, B., Wolf, D., Clayton, R.N., Mayeda, T.K., Sato, T., Suzuki, A., Kojima, H., 2002. Yamato 792947, 793408, and 820038: the most primitive H chondrites, with abundant refractory inclusions. Meteoritics 37, 1417–1434.

Klahr, H.H., Bodenheimer, P., 2002. Turbulence in accretion disks: vorticity generation and angular momentum transport via the global baroclinic instability. Astrophys. J. 582, 869–892.

Krot, A.N., McKeegan, K.D., Leshin, L.A., MacPherson, G.J., Scott, E.R.D., 2002. Existence of an oxygen-16 rich gaseous reservoir in the solar nebula. Science 295, 1051–1054.

Larimer, 1989. The cosmochemical classification of the elements. In: Kerridge, J.F., Matthews, M.S. (Eds.), Meteorites and the Early Solar System. Univ. of Arizona Press, pp. 375–389.

Lawler, M.E., Brownlee, D.E., 1992. CHON as a component of dust from Comet Halley. Nature 359, 810–812.

Lichtenegger, H.I.M., Komlë, N.I., 1991. Heating and evaporation of icy particles in the vicinity of comets. Icarus 90, 319–325.

Lin, D., Papaloizou, J., 1985. On the dynamical origin of the Solar System. In: Black, D.C., Matthews, M.S. (Eds.), Protostars and Planets II. Univ. of Arizona Press, pp. 981–1072.

Lodders, K., Fegley Jr., B., 2002. Atmospheric chemistry in giant planets, brown dwarfs, and low-mass stars. I. Carbon, nitrogen, and oxygen. Icarus 155, 393–424.

Lynden-Bell, D., Pringle, J.E., 1974. The evolution of viscous disks and the origin of the nebular variables. Mon. Not. R. Astron. Soc. 168, 603–637.

Lyons, J.R., Young, E., 2003. Towards an evaluation of self-shielding at the X-point as the source of the oxygen isotope anomaly. In: Proc. Lunar Planet. Sci. Conf. 34th. 1981.pdf.

MacPherson, G.J., Davis, A.M., 1994. Refractory inclusions in the prototypical CM chondrite, Mighei. Geochim. Cosmochim. Acta 58, 5599–5625.

MacPherson, G.J., Wark, D.A., Armstrong, J.T., 1989. Primitive material surviving in chondrites: refractory inclusions. In: Kerridge, J.F., Matthews, M.S. (Eds.), Meteorites and the Early Solar System. Univ. of Arizona Press, pp. 746–807.

Markiewicz, W.J., Mizuno, H., Völk, H.J., 1991. Turbulence-induced relative velocity between two grains. Astron. Astrophys. 242, 286–289.

McKeegan, K.D., Leshin, L.A., Russell, S.S., MacPherson, G.J., 1998. Oxygen isotope abundances in calcium–aluminum rich inclusions from ordinary chondrites: implications for nebula heterogeneity. Science 280, 414–418.

McSween, H., 1977a. Carbonaceous chondrites of the Ornans type: a metamorphic sequence. Geochim. Cosmochim. Acta 41, 477–491.

McSween, H.Y., 1977b. Petrographic variations among carbonaceous chondrites of the Vigarano type. Geochim. Cosmochim. Acta 41, 1777–1790.

Morfill, G.E., Völk, H.J., 1984. Transport of dust and vapor and chemical fractionation in the early protosolar cloud. Astrophys. J. 287, 371–395.

Mostefaoui, S., Kita, N., Togashi, S., Tachibana, S., Nagahara, H., Morashita, Y., 2001. The relative formation ages of ferromagnesian chondrules inferred from their initial aluminum-26/aluminum-27 ratios. Meteorit. Planet. Sci. 37, 421–438.

Mysen, B., Kushiro, I., 1988. Condensation, evaporation, melting, and crystallization in the primitive solar nebula: experimental data in the system MgO–SiO_2–H_2 to 10^{-9} bar and 1870 C with variable oxygen fugacity. Am. Mineral. 73, 1–19.

Nagahara, H., Ozawa, K., 1996. Evaporation of Forsterite in H_2 gas. Geochim. Cosmochim. Acta 60, 1445–1459.

Nagahara, H., Kushiro, I., Mysen, B., 1994. Evaporation of olivine: low pressure phase relations of the olivine system and its implication for the origin of chondritic components of the solar nebula. Geochim. Cosmochim. Acta 58, 1951–1963.

Najita, J., Carr, J.S., Mathieu, R.D., 2003. Gas in the terrestrial planet region of disks: CO fundamental emission from T Tauri stars. Astrophys. J. 589, 931–952.

Nakagawa, Y., Sekiya, M., Hayashi, C., 1986. Settling and growth of particles in a laminar phase of a low-mass solar nebula. Icarus 67, 375–390.

Nittler, L.R., Alexander, C.M.O'D., Giao, X., Walker, R.M., Zinner, E., 1997. Stellar sapphires: the properties and origins of presolar Al_2O_3 in meteorites. Astrophys. J. 483, 475–495.

Prinn, R.G., 1990. On neglect of angular momentum terms in solar nebula accretion disk models. Astrophys. J. 348, 725–729.

Richard, D., 2003. On non-linear hydrodynamic in stability and enhanced transport in differentially rotating flows. Astron. Astrophys. 408, 409–414.

Richard, D., Zahn, J.-P., 1999. Turbulence in differentially rotating flows. What can be learned from the Couette–Taylor experiment. Astron. Astrophys. 347, 734–773.

Ruden, S., Pollack, J.B., 1991. The dynamical evolution of the protosolar nebula. Astrophys. J. 375, 740–760.

Shu, F., Shang, H., Lee, T., 1996. Towards an astrophysical theory of chondrites. Science 271, 1545–1552.

Shukolyukov, A., Lugmair, G.W., 2002. Chronology of asteroid accretion and differentiation. In: Bottke Jr., W.F., Cellino, A., Paolicchi, P., Binzel, R.P. (Eds.), Asteroids III. Univ. of Arizona Press, Tucson, pp. 687–695.

Stevenson, D.J., 1990. Chemical heterogeneity and imperfect mixing in the solar nebula. Astrophys. J. 348, 730–737.

Stepinski, T.F., 1998. The solar nebula as process—an analytic model. Icarus 132, 100–112.

Stepinski, T.F., Valageas, P., 1996. Global evolution of solid matter in turbulent protoplanetary disks. I. Aerodynamics of solid particles. Astron. Astrophys. 309, 301–312.

Stepinski, T.F., Valageas, P., 1997. Global evolution of solid matter in turbulent protoplanetary disks. II. Development of icy planetesimals. Astron. Astrophys. 319, 1007–1019.

Stone, J.M., Gammie, C.F., Balbus, S.A., Hawley, J.F., 2000. Transport processes in protostellar disks. In: Mannings, V., Boss, A.P., Russell, S.S. (Eds.), Protostars and Planets IV. Univ. of Arizona Press, pp. 589–599.

Supulver, K., Lin, D.N.C., 2000. Formation of icy planetesimals in a turbulent solar nebula. Icarus 46, 525–540.

Thiemens, M., 1996. Mass-independent isotopic effects in chondrites: the role of chemical processes. In: Hewins, R., Jones, R., Scott, E.R.D. (Eds.), Chondrules and the Protoplanetary Disk. Cambridge Univ. Press, pp. 107–118. Especially pp. 113–115 on isotopic exchange reactions.

Thiemens, M., 1999. Mass-independent isotope effects in planetary atmospheres and the early Solar System. Science 283, 341–345.

Völk, H.J., Jones, F.C., Morfill, G.E., Röser, S., 1980. Collisions between grains in a turbulent gas. Astron. Astrophys. 85, 316–325.

Weidenschilling, S.J., 1977. Aerodynamics of solid bodies in the solar nebula. Mon. Not. R. Astron. Soc. 180, 57–70.

Weidenschilling, S.J., 1989. Formation processes and timescales for meteorite parent bodies. In: Kerridge, J.F., Matthews, M.S. (Eds.), Meteorites and the Early Solar System. Univ. of Arizona Press, pp. 348–374.

Weidenschilling, S.J., 1997. The origin of comets in the solar nebula: a unified model. Icarus 127, 290–306.

Weidenschilling, S.J., 2000. Formation of planetesimals and accretion of the terrestrial planets. Space Sci. Rev. 92, 295–310.

Weidenschilling, S.J., 2002. Formation of comets. In: Weaver, H.A., Festou, M. (Eds.), Comets II. In press.

Weidenschilling, S., Cuzzi, J.N., 1993. Formation of planetesimals in the solar nebula. In: Levy, E., Lunine, J. (Eds.), Protostars and Planets III. Univ. of Arizona Press.

Wood, J.A., Morfill, G.E., 1989. A review of solar nebula models. In: Kerridge, J.F., Matthews, M.S. (Eds.), Meteorites and the Early Solar System. Univ. of Arizona Press, pp. 329–347.

Wooden, D., 2002. Comet grains; their IR emission and their relation to ISM grains. Earth Moon Planets 89, 247–287.

Woolum, D., Cassen, P.M., 1999. Astronomical constraints on nebular temperatures: implications for planetesimal formation. Meteorit. Planet. Sci. 34, 897–907.

Young, E.D., Lyons, J.R., 2003. CO self-shielding in the outer solar nebula: an astrophysical explanation for the oxygen isotope slope-1 line. In: Proc. Lunar Planet. Sci. Conf. 34th. 1923.pdf.